Three-Dimensional Surface Geophysical Exploration of S/SX Tank Farm

Prepared by **Dale Rucker and Gillian Noonan, Columbia Energy and Environmental Services, Washington River Protection Solutions**
Richland, WA 99352
U.S. Department of Energy Contract DE-AC27-08RV14800

EDT/ECN: DRF UC:
Cost Center: Charge Code:
B&R Code: Total Pages: 52

Key Words: Surface geophysical exploration, SX Farm, Resistivity

Abstract: The report documents the results of a 3D resistivity survey conducted between the 241-S and SX tank farms.

TRADEMARK DISCLAIMER. Reference herein to any specific commercial product, process, or service by trade name, trademark, manufacturer, or otherwise, does not necessarily constitute or imply its endorsement, recommendation, or favoring by the United States Government or any agency thereof or its contractors or subcontractors.

NOV 0 3 2010
DATE:
STA: 15
HANFORD RELEASE
ID: 65

Nancy A Fouad 11/3/2010
Release Approval Date Release Stamp

EXECUTIVE SUMMARY

This report documents surface geophysical exploration (SGE) activities completed within a 96-meter by 90-meter area in the region between S and SX tank farms at the U.S. Department of Energy Hanford Site in Washington State in fiscal year 2010. hydroGEOPHYSICS, Inc. (HGI) and Columbia Energy and Environmental Services, Inc., with support from technical staff of Washington River Protection Solutions, LLC (WRPS), conducted a three-dimensional (3D) electrical resistivity survey of the subsurface. High-resolution electrical resistivity data were acquired using 243 surface electrodes (located at the ground surface), five boreholes containing depth electrodes (24 total depth electrodes), and 15 wells completed within the S-SX tank farm region.

Results of the data processing analyses through comparisons of more than thirty separate inverse models identified several key features of the electrical resistivity distribution of the subsurface:

- Discrete low-resistivity subsurface targets were identified in the model domain. The main body of these targets appeared to be about 20 to 40 meters below ground surface. Given the depth of the target, it is likely that infrastructure had minimal effect on the results.
- Using expert judgment, it is believed that the model with surface and depth electrodes, without long electrodes (Model 024) represents the subsurface most accurately. This is due to the fact that additional subsurface data provided increased sensitivity at depth and gave better resolution to those areas. Plan view depth slices from Inverse Model 024 are provided in Figure ES-1.
- Neutron logging to define volumetric moisture content in the five boreholes, where depth electrodes were placed, shows an increase in moisture at about 25 to 45 meters bgs. The moisture in this region was as high as 30 percent in discrete layers that are about 1 meter thick. Low resistivity targets in the S-SX tank farm area could be attributed to these high moisture regions.

Secondarily, a statistical evaluation of the depth electrodes from B farm, UPR-81, UPR-86, and S-SX tank farms was performed. Key findings from this evaluation include:

- Electrode design has a significant effect on data quality
- Antecedent moisture content did not correlate with electrode performance
- There appears to be a duration following placement of approximately three months when the performance of depth electrodes improves.

Degradation of exposed wire depth electrodes was observed. It is suspected that the applied voltage drives moisture surrounding the electrode off through electrolysis.

Figure ES-1. Plan View Depth Slices of Distribution of Calculated Resistivity for Inverse Model 024_i.

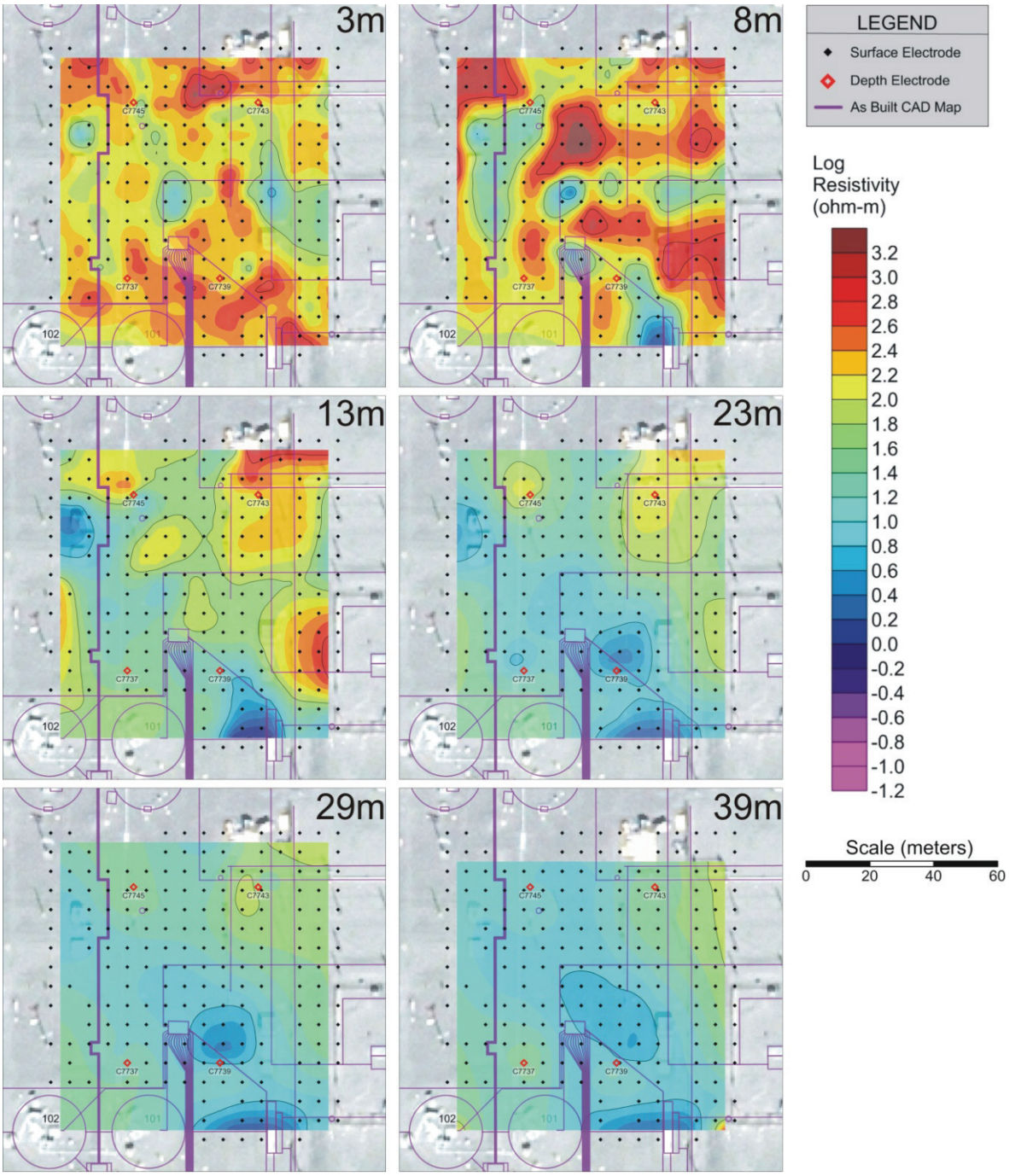

TABLE OF CONTENTS

1.0 INTRODUCTION 1-1
1.1 SCOPE 1-1
1.2 OBJECTIVES 1-1
1.3 REPORT LAYOUT 1-2

2.0 DATA ACQUISITION AND PROCESSING METHODOLOGY 2-1
2.1 SURVEY DESIGN 2-1
2.2 EQUIPMENT 2-4
2.2.1 Electrode and Cable Layout 2-4
2.2.2 Resistivity Meter 2-5
2.3 ACQUISITION METHODOLOGY 2-6
2.4 DATA PROCESSING 2-7
2.4.1 Data Reduction 2-7
2.4.2 3D Inverse Modeling 2-10

3.0 STATISTICAL EVALUATION OF DEPTH ELECTRODES 3-1
3.1 CONSTRUCTION AND COMPLETION DETAILS 3-2
3.2 DATA ACQUISITION WITH DEPTH ELECTRODES 3-8
3.3 CHRONOAMPEROMETRY 3-12

4.0 PRELIMINARY MODELING RESULTS 4-1
4.1 INVERSE MODELING RESULTS 4-1
4.1.1 Surface to Surface Only 4-1
4.1.2 Surface-to-Surface with Depth Electrodes 4-5
4.1.3 Surface, Depth, and Long Electrodes 4-8
4.2 MODELING PERFORMANCE 4-11

5.0 CONCLUSIONS AND RECOMMENDATIONS 5-1
5.1 DEPTH ELECTRODE ANALYSIS 5-1
5.2 SUBSURFACE CHARACTERIZATION 5-2

6.0 REFERENCES 6-1

LIST OF FIGURES

1-1. Color Contoured Results from Previous Surface-to-Surface SGE Results at SX Farm Showing Location of Current Survey in Red. 1-3
2-1. Electrode Layout and the Local Distribution of Infrastructure for the S-SX Tank Farm Survey Area 2-2
2-2. Resistivity Data Acquisition System 2-5
2-3. Forward and Reverse Data Sets (Raw Data) 2-8

2-4. Forward and Reverse Data Sets after Data Editing 2-9
3-1. Multi-Probe Depth Electrode Example 3-6
3-2. Multi-Core Cable with Steel Braid Depth Electrode Example 3-7
3-3. Performance Measure for Each of the Depth Electrodes 3-11
3-4. Temporal Performance of a Stable Electrode 3-14
3-5. Temporal Performance of a Unstable Electrode 3-14
3-6. Temporal Performance of a Unstable Electrode 3-15
4-1. Distribution of Calculated Resistivity for Inverse Model 001_ii 4-2
4-2. Neutron Logging Moisture Data from C7739 4-3
4-3. Plan View Depth Slices of Distribution of Calculated Resistivity for Inverse Model 001_ii 4-4
4-4. Distribution of Calculated Resistivity for Inverse Model 024_i 4-6
4-5. Plan View Depth Slices of Distribution of Calculated Resistivity for Inverse Model 024_i 4-7
4-6. Distribution of Calculated Resistivity for Inverse Model 026_i 4-9
4-7. Plan View Depth Slices of Distribution of Calculated Resistivity for Inverse Model 026_i 4-10
4-8. Model 001 Convergence Curve 4-11
4-9. Model 024 Convergence Curve 4-12
4-10. Model 026 Convergence Curve 4-13

LIST OF TABLES

2-1. Depth Electrode Locations 2-2
2-2. Well Locations 2-3
2-3. Number of Data Points Retained During Data Editing Steps 2-9
3-1. Depth Electrode Details for B Tank Farm. 3-2
3-2. Depth Electrode Details for BX Tank Farm. 3-3
3-3. Depth Electrode Details for UPR-81 near C Tank Farm. 3-3
3-4. Depth Electrode Details for UPR-86 near C Tank Farm. 3-4
3-5. Depth Electrode Details for S/SX Tank Farm. (2 Sheets) 3-4
3-6. Depth Electrode Data from All Projects 3-9
3-7. Depth Electrode Time Differential from All Projects 3-11
4-1. Inverse Modeling Convergence and Error Statistics 4-13

LIST OF TERMS

Δm	modeled resistivity
2D	two-dimensional
3D	three-dimensional
AGI	Advanced Geosciences, Inc.
bgs	below ground surface
DTS	depth-to-surface
GPS	Global Positioning System
HGI	hydroGEOPHYSICS, Inc.
RMS	root-mean-square
SGE	surface geophysical exploration
STS	surface-to-surface
UPR	unplanned release
V/I	resistance
WRPS	Washington River Protection Solutions, LLC
WTS	well-to-surface

Units

ft	feet
in.	inch(es)
m	meter(s)
mA	milliamp

1.0 INTRODUCTION

This report documents surface geophysical exploration (SGE) activities completed within a 96-meter by 90-meter area in the region between S and SX tank farms at the U.S. Department of Energy Hanford Site in Washington State in fiscal year 2010. hydroGEOPHYSICS, Inc. (HGI) and Columbia Energy and Environmental Services, Inc., with support from technical staff of Washington River Protection Solutions, LLC (WRPS), conducted a three-dimensional (3D) survey of the subsurface using electrical resistivity. Data acquisition and analysis were performed in accordance with RPP-PLAN-45906, *Work Plan for Surface Geophysical Exploration of the S and SX Tank Farms at the Hanford Site.* High-resolution electrical resistivity data were acquired using 243 surface electrodes (located at the ground surface), five boreholes containing depth electrodes (24 total depth electrodes), and 15 wells completed within the S-SX tank farm region.

1.1 SCOPE

The scope of this electrical resistivity characterization survey included:

- Data acquisition on surface electrodes, depth electrodes, and wells
- Statistical evaluation of depth electrodes to ensure quality in data acquisition
- Compilations of 3D resistivity cross sections of the region between S-SX tank farms.

1.2 OBJECTIVES

The primary objective of the S-SX farm SGE survey was to refine the current understanding of the location of low-resistivity features that can be used to support planning for the location and size of an interim surface barrier. Characterization was performed in FY 2009 because of large historic leaks of tank waste in that farm. The results of the previous surface-to-surface (STS) SGE survey at the S and SX tank farms (RPP-RPT-42513, *Surface Geophysical Exploration of the SX Tank Farm at the Hanford Site*) identified a low resistivity anomaly northeast of SX tank farm as shown in Figure 1-1. The low resistivity anomaly was interpreted as a possible indicator that soil contamination may exist in the region between 241-SX and 241-S farms, near the catch tank 241-SX-302 and diversion box 241-SX-152. The leak loss evaluation report for Waste Management Area S/SX (RPP-ENV-39658, *Hanford SX-Farm Leak Assessments Report*) indicated historic evidence of pipeline leaks in this area. Additionally, drilling results in this area showed increased moisture, prompting further investigation. As a result of this information, a decision was made to perform additional resistivity characterization in the area southeast of 241-S farm and northeast of 241-SX farm, near the catch tank/diversion box.

1.3 REPORT LAYOUT

The overall scope and content of this report is divided into several main sections as follows:

- **Section 1.0, Introduction** – Describes the scope and objectives of the investigation.
- **Section 2.0, Data Acquisition and Processing** – Presents general layout of the data acquisition and processing with methods and controls used to ensure the quality and control of data collection, reduction, and processing used in this study.
- **Section 3.0, Statistical Evaluation of Depth Electrodes** – A data analysis on the performance of different types of depth electrodes used in the B, C, and S-SX tank farms.
- **Section 4.0, Preliminary Modeling Results** – Presents the preliminary modeling results from the electrical resistivity surveying effort.
- **Section 5.0, Conclusions** – Provides a summary and conclusions drawn from the results. Recommendations for future depth electrode installation is provided.
- **Section 6.0, References** – Provides a listing of references cited in the report.

Figure 1-1. Color Contoured Results from Previous Surface-to-Surface SGE Results at SX Farm Showing Location of Current Survey in Red.

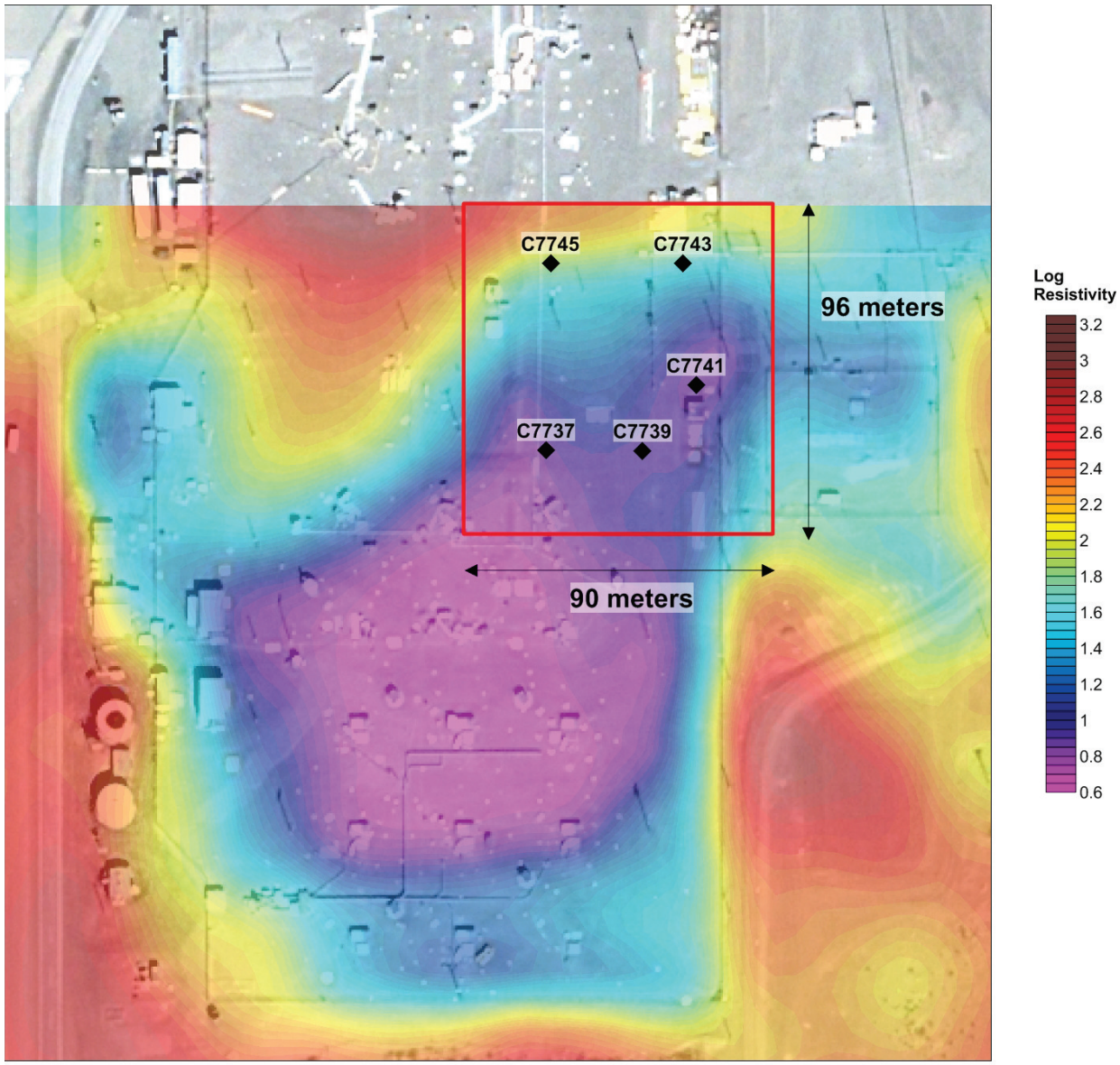

Source: RPP-RPT-42513.

2.0 DATA ACQUISITION AND PROCESSING METHODOLOGY

Data acquisition for a 3D electrical resistivity survey at the S-SX tank farm began on June 17, 2010, and was completed on June 20, 2010. The geophysical survey was initiated to collect data on surface electrodes, electrodes buried deeply beneath the surface (i.e., depth electrodes), and wells. The 3D methodology is in contrast to most previous SGE surveys, where data acquisition was relegated to sets of parallel and orthogonal two-dimensional (2D) profiles collected along individual lines, which when grouped together produce a 3D image. A 3D survey is superior to a 2D survey because considerably more data are collected to define the electrical properties of the subsurface. However, 3D surveys usually take longer to acquire and require more resistivity equipment.

Data collection activities, along with the basis and selection of data collection equipment, and data processing are described in the following sections.

2.1 SURVEY DESIGN

Resistivity data were collected based on a 3D data acquisition method that made use of different electrode arrangements. The surface electrodes were distributed across a uniform grid to optimize the inversion models used in the data analysis and interpretation. The significantly larger amounts of data associated with a 3D survey, relative to a 2D survey, makes an optimized geometry crucial to reduce modeling run times and analysis. For the S-SX tank farm survey, 243 surface electrodes were distributed across a site 96 meters by 90 meters, with electrodes spaced nominally every 6 meters in the east-west and north-south direction. Some positions along this grid were skipped based on the proximity to near surface infrastructure or surface obstructions.

Further resolution is possible by adding depth electrodes to a surface electrode geometry, whereby electrical current and voltage measurements can be made near or within a target. Depth electrodes have the added benefit of being further from near-surface infrastructure and associated electrical interference and noise. For the S-SX tank farm survey, five boreholes with nested depth electrodes labeled C-7737, C-7739, C-7741, C-7743 and C-7745 were placed opportunistically, that is, in areas devoid of surface infrastructure. The footprint of the depth electrodes did not necessarily align to the surface grid. Table 2-1 displays the locations and depths associated with each depth electrode.

The S-SX tank farm 3D survey was also the first to include wells as long electrodes in combination with depth and surface electrodes. The wells were located along the periphery of the site with six wells in the north associated with the S farm, eight wells in the south associated with SX farm (well 299-W22-54 was not used), and two wells between the farms. Table 2-2 lists the specific wells for the survey.

Figure 2-1. Electrode Layout and the Local Distribution of Infrastructure for the S-SX Tank Farm Survey Area.

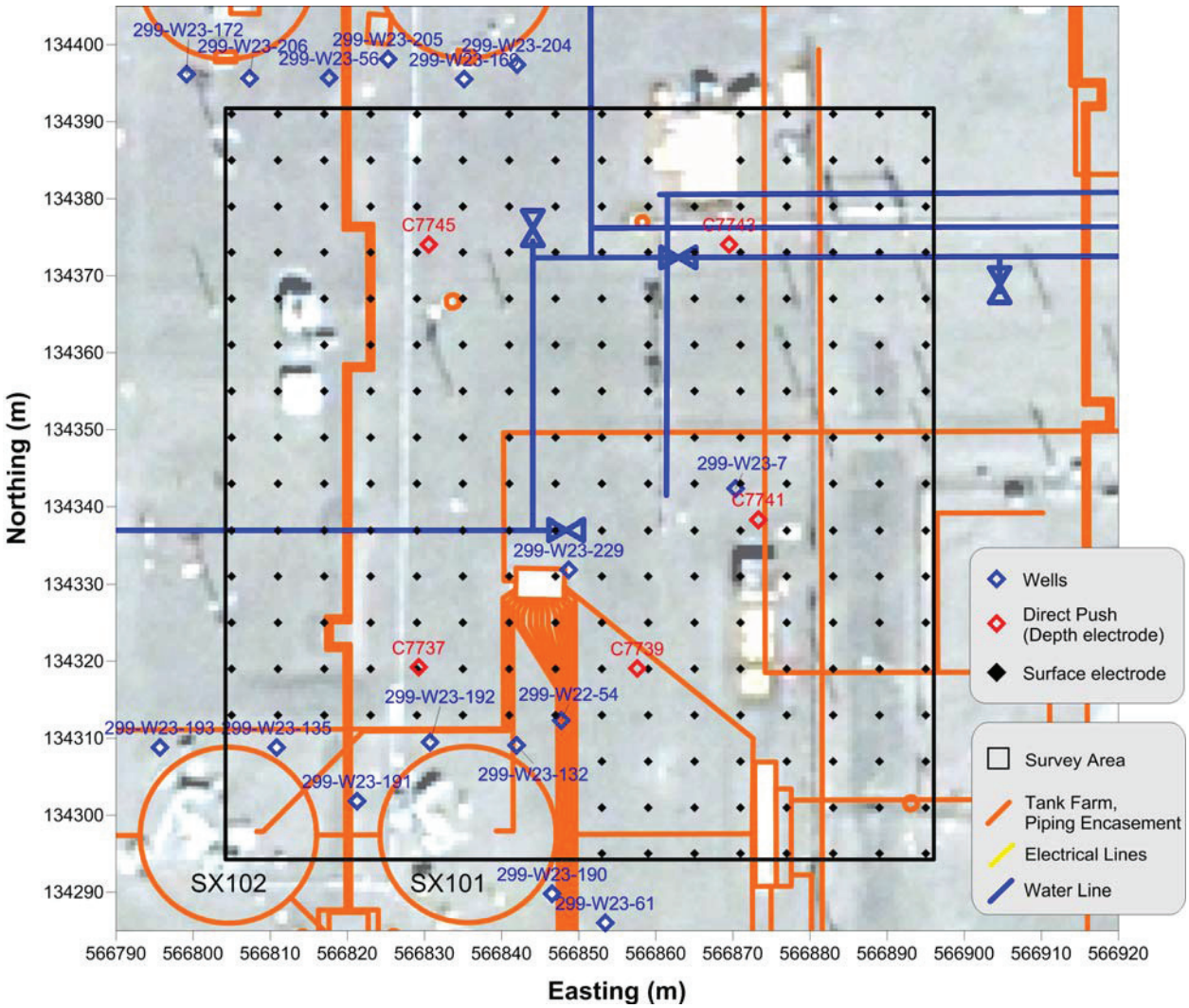

North is located at the top of the figure.

Table 2-1. Depth Electrode Locations. (2 Sheets)

Probe Hole #	Electrode #	Northing (m)	Easting (m)	Electrode Depth (m)	Electrode Depth (ft)
C7737	C7737-60	566829.3	134319.2	18.29	60
	C7737-80			24.38	80
	C7737-100			30.48	100
	C7737-120			36.58	120
	C7737-140			42.67	140

Table 2-1. Depth Electrode Locations. (2 Sheets)

Probe Hole #	Electrode #	Northing (m)	Easting (m)	Electrode Depth (m)	Electrode Depth (ft)
–	C7737-159	–	–	48.46	159
C7739	C7739-93	566857.6	134319.1	28.35	93
–	C7739-113	–	–	34.44	113
–	C7739-133	–	–	40.54	133
–	C7739-152	–	–	46.33	152
C7741	C7741-33	566873.3	134338.4	10.06	33
–	C7741-53	–	–	16.15	53
–	C7741-133	–	–	40.54	133
–	C7741-152	–	–	46.33	152
C7743	C7743-36	566869.5	134374.1	10.97	36
–	–	–	–	29.57	97
C7745	C7745-10	566830.6	134374.1	3.17	10
–	C7745-31	–	–	9.31	31
–	C7745-51	–	–	15.41	51
–	C7745-71	–	–	21.52	71
–	C7745-91	–	–	27.61	91
–	C7745-111	–	–	33.68	111
–	C7745-153	–	–	46.63	153

Table 2-2. Well Locations. (2 Sheets)

Well Name	Tank Farm	Easting (m)	Northing (m)	Casing Length (m)
299-W23-172	S	566799.1	134396.1	31
299-W23-206	S	566807.4	134395.6	30
299-W23-56	S	566817.7	134395.6	46
299-W23-205	S	566825.3	134398.1	31
299-W23-169	S	566835.1	134395.5	44
299-W23-204	S	566842	134397.4	30
299-W23-61	SX	566853.5	134286	30
299-W23-190	SX	566846.5	134289.8	31
299-W23-193	SX	566795.7	134308.8	30
299-W23-135	SX	566810.8	134308.8	43
299-W23-191	SX	566821.3	134301.9	31
299-W23-192	SX	566830.7	134309.5	31
299-W23-132	SX	566842	134309	43

Table 2-2. Well Locations. (2 Sheets)

Well Name	Tank Farm	Easting (m)	Northing (m)	Casing Length (m)
299-W23-229	Between S/SX	566848.7	134331.8	30
299-W23-7	Between S/SX	566870.3	134342.3	30

2.2 EQUIPMENT

2.2.1 Electrode and Cable Layout

The first stage of the project was to assemble all available infrastructure maps for the S-SX tank farm area. The resulting maps were combined into an AutoCAD® drawing and subsequently used to define the coordinates for electrode placement. The maps containing infrastructure locations, including subsurface pipes/structures and surface structures, were digitized and combined with the electrode locations. Electrode locations was then modified to avoid being directly over infrastructure where possible. Placement of electrodes were limited by maintaining a uniform 6-meter grid layout to support data processing software. The final electrode layout was then uploaded into a Leica® 1200 Global Positioning System (GPS) which was used to mark locations on the ground surface. The Leica system has sub-centimeter accuracy, assuring the survey geometry will remain intact.

The electrodes are connected to the resistivity acquisition meter by way of multi-cored cables and multiplexors. For the S-SX project, a total of four cables were deployed, with each cable allowing up to 84 electrodes. The cables were placed in a serpentine pattern with cable offset of 12 meters in the east-west direction. Jumpers were then used to connect to electrodes on a 6-meter basis. In some areas, the specific location of the cable was modified to accommodate the tanks. Figure 2-2 shows the cable and electrode layout used for this project.

Six 56-electrode switch boxes (multiplexors), manufactured by Advanced Geosciences, Inc. (AGI), acted as junction boxes to connect the resistivity meter to the ground cables. The multiplexors provided a 336 electrode capability, of which 243 were used for surface electrodes, 24 for depth electrodes, and 15 wells. A separate patch panel was used to connect the depth electrodes to the multiplexor.

® AutoCAD is a registered trademark of AutoDesk, Inc.
® Leica is a registered trademark of Leica Technology.

Figure 2-2. Resistivity Data Acquisition System.

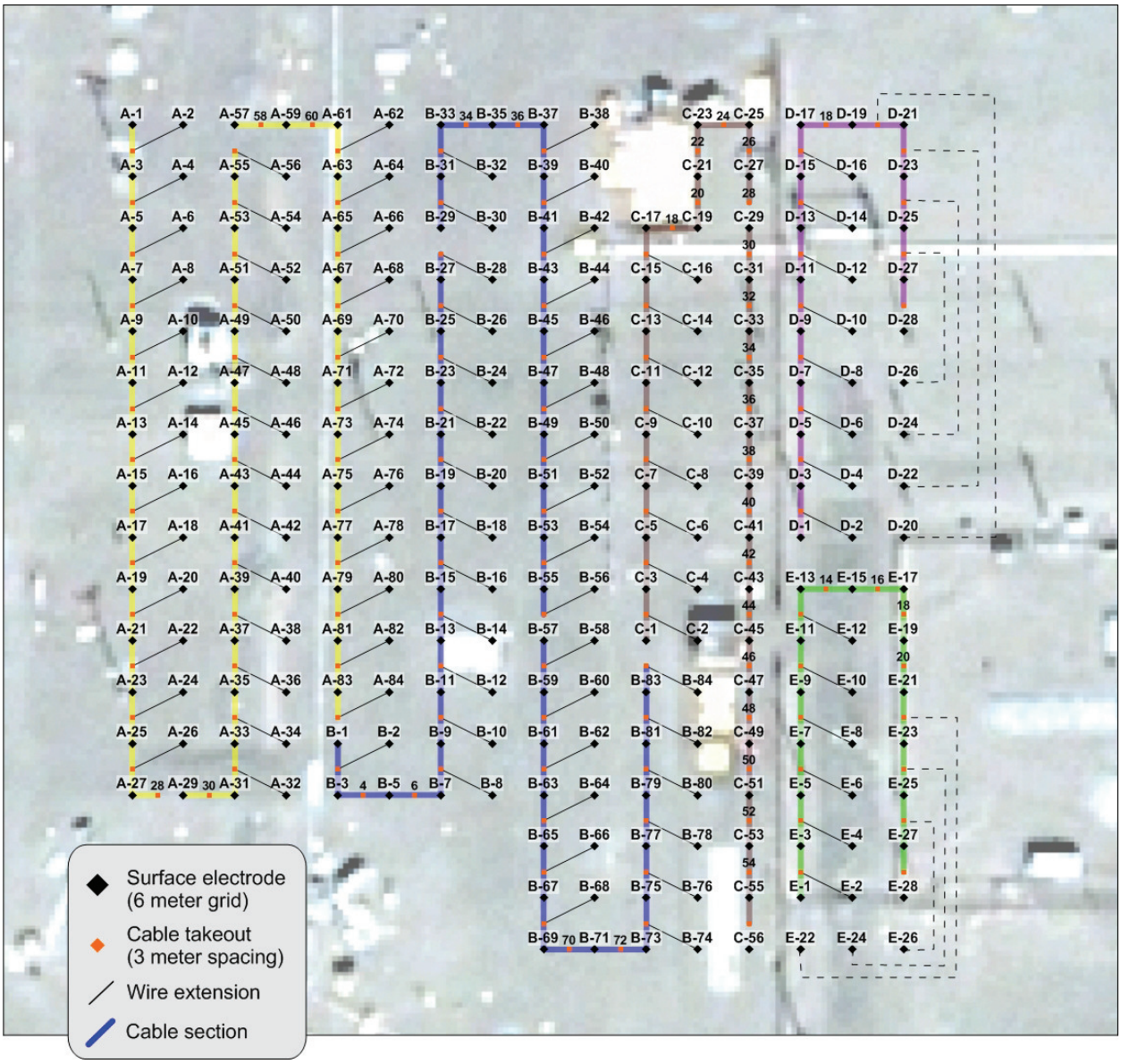

2.2.2 Resistivity Meter

A (SuperSting R8®) resistivity meter, manufactured by AGI, was used for resistivity data acquisition. The meter is capable of full 8-channel acquisition, whereby eight simultaneous measurements of voltage can be made during electrical current transmission. The R8 meter has been used for many SGE projects and has proven itself to be reliable for long-term, continuous acquisition campaigns.

® SuperSting R8 is a registered trademark of Advanced Geosciences, Inc.

Intensive quality assurance was completed before and after the survey to ensure the equipment was functioning appropriately as well as the quality of data was acceptable. Calibration requirements are described for hardware used to collect geophysical data in CEES-0360, *Surface Geophysical Exploration System Design Description*. As an example, the manufacturer (AGI) of the resistivity data acquisition instrument recommends a yearly calibration of internal calibration resistors. The calibration is performed at the manufacturer's facility and a certificate of calibration is provided. A copy of the calibration documentation, serial numbers, and expiration dates are maintained in project files.

Daily inspection of the receiver calibration was also performed onsite using the manufacturer-supplied calibration resistor test box. The supplied test box is connected to the SuperSting R8 before commencing the daily survey. A specific calibration test firmware is provided within the SuperSting and provides the operator with a pass/fail indication for each of the eight receiver channels. If any of the channels fail, a recalibration or repair is required.

2.3 ACQUISITION METHODOLOGY

The resistivity acquisition included a pole-pole array, where one electrode from each of the transmitting and receiving electrode pairs were placed effectively at infinity. Practically, these poles are placed remotely, anywhere from 2 to 5 times the maximum internal electrode distance away from the site in opposite directions.

Data collection was initialized on June 17, 2010, and completed June 20, 2010, with approximately 71 hours of near-continuous acquisition. Operations were interrupted briefly to perform the daily inspection of the resistivity meter. Data were collected around the clock, 24 hours a day over a long weekend to minimize impacts to tank farm operations. Additionally, continuous data collection was used to minimize the influence of changing moisture conditions over longer periods of time. Personnel were maintained onsite at all times to monitor data collection and to keep the cable area clear of vehicles and equipment that could damage equipment and impact data quality.

Both forward and reverse data sets were collected during data acquisition in order to increase the resolution of the resistivity survey and evaluate data quality. Forward and reverse measurements are acquired by switching the transmitting and receiving electrodes to produce a reciprocal dataset. The two sets of data ensured that each electrode acted as both transmitter and receiver; both are needed for quality control. The theory of reciprocity implies that a homogeneous earth should allow for consistent measurements in both forward and reverse measurement conditions. Thus, by varying selected reciprocal percent difference thresholds, the ratio between data quality and quantity can be assessed. For this survey effort, data measurements with a relative percent difference greater than 5 percent were considered unacceptable and removed from the dataset before numerical inverse modeling.

2.4 DATA PROCESSING

2.4.1 Data Reduction

All raw data collected at the site were compiled into a relational database. Raw data included both electrical resistivity data and GPS positional data to geo-reference the resistivity data. A set of queries was designed to segregate reciprocal pair data points and assign each data point distinguishing characteristics not retained in the raw sting file. This information included electrode type and a sequential electrode number (as designated in the survey design). Additional data fields were added for the calculated distance between electrodes and percent error between reciprocal data. The data were then exported from the database for graphical filtering and plotting in a spreadsheet.

Four important diagnostic data parameters from the raw data include voltage/current (V/I; resistance), repeat error, reciprocal error, and electrical current output. The repeat error is a calculated percent error between cycled/repeated measurements. A plot of these data can provide information with regards to the statistical variation of the data population.

The process of data editing identifies and eliminates data points, but no data modification (rounding, averaging, smoothing, or splining) is permitted. The rationale is to seek out and remove spurious points that do not conform to the data population or points that violate potential theory. The first step in this editing process was to remove data outside of the statistical population – negative V/I, noise, high instrument error, low current, low voltage, etc. Figure 2-3 shows the raw data distribution of the forward and reverse data, while Figure 2-4 shows the same datasets after filtering. The next step in data reduction was to apply a data quality filter based on reciprocity. All data with a reciprocal percent difference greater than 5 percent was removed.

Figure 2-3. Forward and Reverse Data Sets (Raw Data).

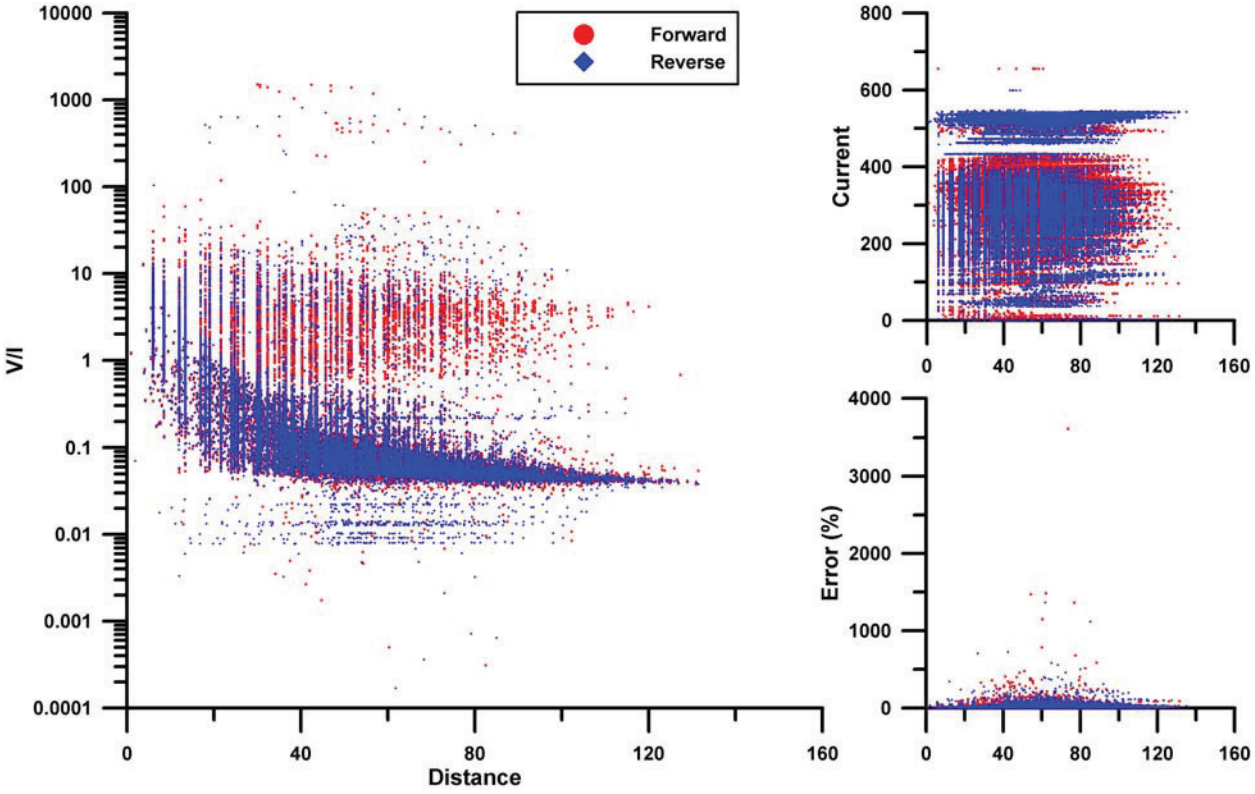

Raw data distribution for (1) V/I (left), (2) Error, and (3) Current (lower right).
All are plotted against the distance between transmitting/receiving electrode pairs.

Figure 2-4. Forward and Reverse Data Sets after Data Editing.

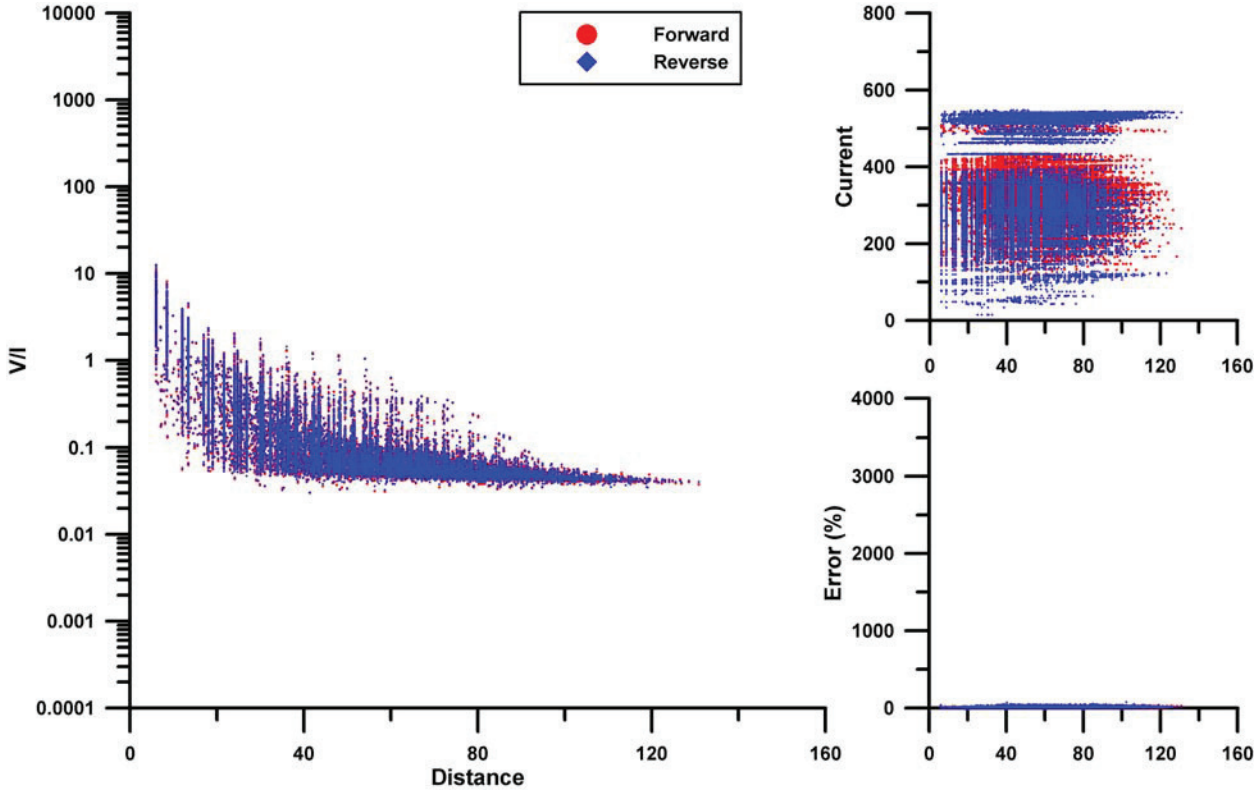

Data distribution after Editing for (1) V/I (left), (2) Error, and (3) Current (lower right).
All are plotted against the distance between transmitting/receiving electrode pairs.

Table 2-3 displays the percentages of data removed or retained during steps of the editing process.

Table 2-3. Number of Data Points Retained During Data Editing Steps.

	Forward	Reverse	Sum	Percent of Total
Total Raw	38,420	38,172	76,592	100%
Total Combined Reciprocal	27,313	27,313	54,626	71.3%
Total Edited	18,156	18,156	36,312	47.4%

2.4.2 3D Inverse Modeling

Popular use of the RES3D series of resistivity inversion codes has led both professional and academic users to regard these codes as industry standard software. The S-SX tank farm modeling effort used RES3DINVx64, a 64-bit multi-threaded version developed specifically for a large number of electrodes.

In general, inverse modeling can be summarized in the following five steps.

1. The study site's voltage data has been measured and is discretized into grid nodes using a finite difference or finite element mesh. The meshing parameters used in either case, to design the computational grids, are dependent on electrode spacing used in site-specific data acquisition.
2. The inversion will set out to estimate the true resistivity at every grid node. An initial estimate of the subsurface properties is made based on the literal translation of the pseudo-section to a true resistivity, a constant value, or some other distribution from *a-priori* information. A forward model run with these initial estimates is made to obtain the distribution of voltages in the subsurface. The root-mean-square (RMS) error is calculated between the measured voltage and the calculated voltage resulting from the forward run.
3. Based on the degree of model fit to field measurements, the initial estimate of resistivity is changed to improve the overall model fit and the forward model with the updated estimates is rerun. The iterative method linearizes a highly nonlinear problem using Newton's method. Using this method, the inverse modeling code essentially solves the linearized problem to obtain the change in modeled resistivity (Δm) for the next iteration.
4. The resistivity model is updated using the general formula $m_{i+1} = m_i + \Delta m$, where $_{mi+1}$ is the resistivity in a model cell at the next iteration, and m_i is the current value.
5. Steps 3 and 4 are repeated until the RMS error change between successive iterations reaches an acceptable level.

3.0 STATISTICAL EVALUATION OF DEPTH ELECTRODES

Since the inception of the SGE program at Hanford, great effort has been expended to increase the utility of electrical resistivity measurements to define the location of waste plumes. One method to increase the utility has been in the area of data acquisition and electrode geometry. The first test for SGE was the T tank farm (RPP-RPT-28955, *Surface Geophysical Exploration of T Tank Farm*) in 2005, where electrodes were placed on the surface along parallel and orthogonal line sets. The data acquired inside the tank farm fence was of marginal quality, and it was recommended that wells be used as long electrodes. The final report demonstrated success with long electrodes but additional recommendations were provided for increased resolution of targets inside the farm through the use of buried point source electrodes or vertical nested array of electrodes.

Drilling inside the tank farm fence can be expensive, so opportunistic methods were developed to place single depth electrodes during direct push sampling. A single electrode was placed in the hole after a sacrificial tip was disconnected from the drill string. The metallic tip proved to be a good electrode at a relatively low cost and the method was first applied in late 2006 at the B and BX tank farms (RPP-34690, *Surface Geophysical Exploration of B, BX, and BY Tank Farms at the Hanford Site)*. For this application, eight depth electrodes were connected to the resistivity meter along with several individual resistivity lines to acquire a depth-to-surface (DTS) dataset. Since this time, depth electrodes have been used actively for the following SGE projects:

- Unplanned Release (UPR)-81 in 2009 (RPP-RPT-41236, *Surface Geophysical Exploration of UPR 200-E-81 Near the C Tank*)
- UPR-82 in 2010 (RPP-RPT-47486, *Surface Geophysical Exploration of UPR 200-E-86 Near the C Tank*)
- S/SX tank farm in 2010 (this project).

Additionally, depth electrodes have been placed in other tank farms in anticipation of upcoming SGE projects:

- C tank farm
- BY tank farm
- U tank farm.

Regardless of electrode type, some electrodes perform better than others in terms of outputting high electrical current and making accurate and repeatable voltage measurements. Their performances typically rely on the environmental setting, mode of placement, and in the case of depth electrodes, mode of well completion and electrode construction. Conventionally, electrodes perform the best when constructed of a low polarizable material, with high surface area, and in contact with low resistivity earth. Stainless steel is often used as the construction material based on longevity and low corrosion, although other electrode types, such as copper-copper sulfate electrodes, may perform better (Labrecque and Daily, 2008). To decrease the earth resistance around the electrode (also called contact resistance), water and sometimes salt is

added to the well at the electrode's position. According to Ohm's law, a lower contact resistance will result in a higher output current.

Given the low density of depth electrodes at a given site, where typically 4 to 24 electrodes are placed below ground surface (bgs) (compared to hundreds of electrodes on the surface), it is important to have maximum performance from all depth electrodes. Unfortunately, many of the electrodes for this S/SX tank farm project were found to be impaired in their ability to transmit electrical current and provided low accuracy and low repeatability in the voltage measurements. It appeared that a larger percentage of data from these electrodes were removed from the population during the editing phase compared to past projects. The impairment could have been related to the electrode construction or well completion, because a variety of electrode construction and completion methods were employed for the project. A detailed investigation into the performance from this and past projects is presented below to help understand how best to maximize usage from the depth electrodes for future projects.

3.1 CONSTRUCTION AND COMPLETION DETAILS

The construction and completion details for the depth electrodes of the different completed SGE projects are provided in Tables 3-1, 3-2, 3-3, 3-4, and 3-5.

Table 3-1. Depth Electrode Details for B Tank Farm.

Electrode Name	C5161	C5165	C5177	C5179
Construction Type	Single-Probe	Single-Probe	Single-Probe	Single-Probe
Date of Construction	12/2006 to 1/2007	12/2006 to 1/2007	12/2006 to 1/2007	12/2006 to 1/2007
Depth of Probes (ft)	55	55	35	35
Construction Details	Single stainless steel rod electrode, 2 ft long, 0.5 in. diameter. 16 gauge wire connection to the surface	Single stainless steel rod electrode, 2 ft long, 0.5 in. diameter. 16 gauge wire connection to the surface	Single stainless steel rod electrode, 2 ft long, 0.5 in. diameter. 16 gauge wire connection to the surface	Single stainless steel rod electrode, 2 ft long, 0.5 in. diameter. 16 gauge wire connection to the surface
Fill Material	Silica sand and saline water surround probe, bentonite fill	Silica sand and saline water surround probe, bentonite fill	Silica sand and saline water surround probe, bentonite fill	Silica sand and saline water surround probe, bentonite fill

Table 3-2. Depth Electrode Details for BX Tank Farm.

Electrode Name	C5125	C5129	C5131	C5135
Construction Type	Single-Probe	Single-Probe	Single-Probe	Single-Probe
Date of Construction	12/2006 to 1/2007	12/2006 to 1/2007	12/2006 to 1/2007	12/2006 to 1/2007
Depth of Probes (ft)	50	78	50	78
Construction Details	Single stainless steel rod electrode, 2 ft long, 0.5 in. diameter. 16 gauge wire connection to the surface	Single stainless steel rod electrode, 2 ft long, 0.5 in. diameter. 16 gauge wire connection to the surface	Single stainless steel rod electrode, 2 ft long, 0.5 in. diameter. 16 gauge wire connection to the surface	Single stainless steel rod electrode, 2 ft long, 0.5 in. diameter. 16 gauge wire connection to the surface
Fill Material	Silica sand and saline water surround probe, bentonite fill	Silica sand and saline water surround probe, bentonite fill	Silica sand and saline water surround probe, bentonite fill	Silica sand and saline water surround probe, bentonite fill

Table 3-3. Depth Electrode Details for UPR-81 near C Tank Farm.

Electrode Name	C6395	C6399
Construction Type	Dual-Probe	Dual-Probe
Date of Construction	5/08/08 to 6/30/08	4/22/08 to 6/25/2008
Depth of Probes (ft)	50, 146	50, 215
Construction Details	Multiple stainless steel rod electrode, 2 ft long, 0.5 in. diameter. 16 gauge wire connection to the surface	Multiple stainless steel rod electrode, 2 ft long, 0.5 in. diameter. 16 gauge wire connection to the surface
Fill Material	silica sand and saline water surround probe, filled with bentonite	silica sand and saline water surround probe, filled with bentonite

Table 3-4. Depth Electrode Details for UPR-86 near C Tank Farm.

Electrode Name	C5943	C5947	C5957	C5959	C5963
Construction Type	Single-Probe	Single-Probe	Single-Probe	Single-Probe	Single-Probe
Date of Construction	11/5/07 to 2/25/08	11/1/07 to 2/25/08	11/27/07 to 2/25/08	11/20/07 to 3/19/08	11/06/07 to 3/19/08
Depth of Probes (ft)	90	150	143	95	95
Construction Details	Single stainless steel rod electrode, 2 ft long, 0.5 in. diameter. 16 gauge wire connection to the surface	Single stainless steel rod electrode, 2 ft long, 0.5 in. diameter. 16 gauge wire connection to the surface	Single stainless steel rod electrode, 2 ft long, 0.5 in. diameter. 16 gauge wire connection to the surface	Single stainless steel rod electrode, 2 ft long, 0.5 in. diameter. 16 gauge wire connection to the surface	Single stainless steel rod electrode, 2 ft long, 0.5 in. diameter. 16 gauge wire connection to the surface
Fill Material	Silica sand and saline water surround probe, bentonite fill	Silica sand and saline water surround probe, bentonite fill	Silica sand and saline water surround probe, bentonite fill	Silica sand and saline water surround probe, bentonite fill	Silica sand and saline water surround probe, bentonite fill

Table 3-5. Depth Electrode Details for S/SX Tank Farm. (2 Sheets)

Electrode Name	C7737	C7739	C7741	C7743	C7745
Construction Type	Multi-Probe, New WRPS	Multi-Probe, New WRPS	Multi-Probe, New WRPS	Dual-Probe	Multi-Probe, HGI
Date of Construction	2/10	2/10	2/10	3/10	3/10
Depth of Probes (feet)	159, 140, 120, 80, 60, 40, 11	152, 133, 113, 93, 73, 53, 33	152, 133, 113, 93, 73, 53, 33	97, 36	153, 110, 70, 90, 50, 30, 10
Construction Details	Multi-probe depth electrode array that essentially is comprised of exposed 16 gauge wire from a multi-core cable without an electrode (limited surface area) and completed with dry sand with salt added around the electrode with bentonite plugs	Multi-probe depth electrode array that essentially is comprised of exposed 16 gauge wire from a multi-core cable without an electrode (limited surface area) and completed with dry sand with salt added around the electrode with bentonite plugs	Multi-probe depth electrode array that essentially is comprised of exposed 16 gauge wire from a multi-core cable without an electrode (limited surface area) and completed with dry sand with salt added around the electrode with bentonite plugs	Dual probe with a saturated sand/salt completion Probes approximately 2 ft long, 0.5-in. diameter, placed at the bottoms and midway in the borehole	A multi-core cable with steel braid used as an electrode with wet diatomaceous earth around the electrodes and bentonite plug between electrodes (see Figure 3-2).

Table 3-5. Depth Electrode Details for S/SX Tank Farm. (2 Sheets)

Electrode Name	C7737	C7739	C7741	C7743	C7745
	between electrodes (see Figure 3-1)	between electrodes (see Figure 3-1)	between electrodes (see Figure 3-1)		
Fill Material	Sand (10-20) mixed with salt to surround probe, bentonite fill	Sand (10-20) mixed with salt to surround probe, bentonite fill	Sand (10-20) mixed with salt to surround probe, bentonite fill	Sand (10-20) saturated with salt water to surround probe, bentonite fill	Sand (20-40) and diatomite surround moisture probe, water added through tremie. Fill of bentonite, sand and diatomaceous earth

Note: Date of construction based on geophysical borehole logging date.

In summary, the first depth electrodes to be placed in and around tank farms were the single probe completed with sand and saline water around the probed to ensure low contact resistance with the ground. A bentonite plug was used to complete the well to the surface. A water resistant cover is then placed over the wire leads for long term protection from environmental degradation. The single probe construction included B tank farm, BX tank farm, and UPR-86. Around April 2008, the switch was made to use two depth electrodes in each hole, starting with UPR-81. The well completion was similar as the single probe. The most recent work in S-SX shows several different types of depth electrodes and completion methods including:

1. The dual probe with a saturated sand/salt completion for C7743;
2. A multi-probe depth electrode array that essentially is comprised of exposed 16 gauge wire from a multi-core cable without an electrode (limited surface area) as shown in Figure 3-1 and completed with dry sand with salt added (C7737, C7739, and C7741) around the electrode with bentonite plugs between electrodes, and
3. A multi-core cable with steel braid used as an electrode as shown in Figure 3-2 with wet diatomaceous earth around the electrodes and bentonite plug between electrodes.

Figure 3-1. Multi-Probe Depth Electrode Example.

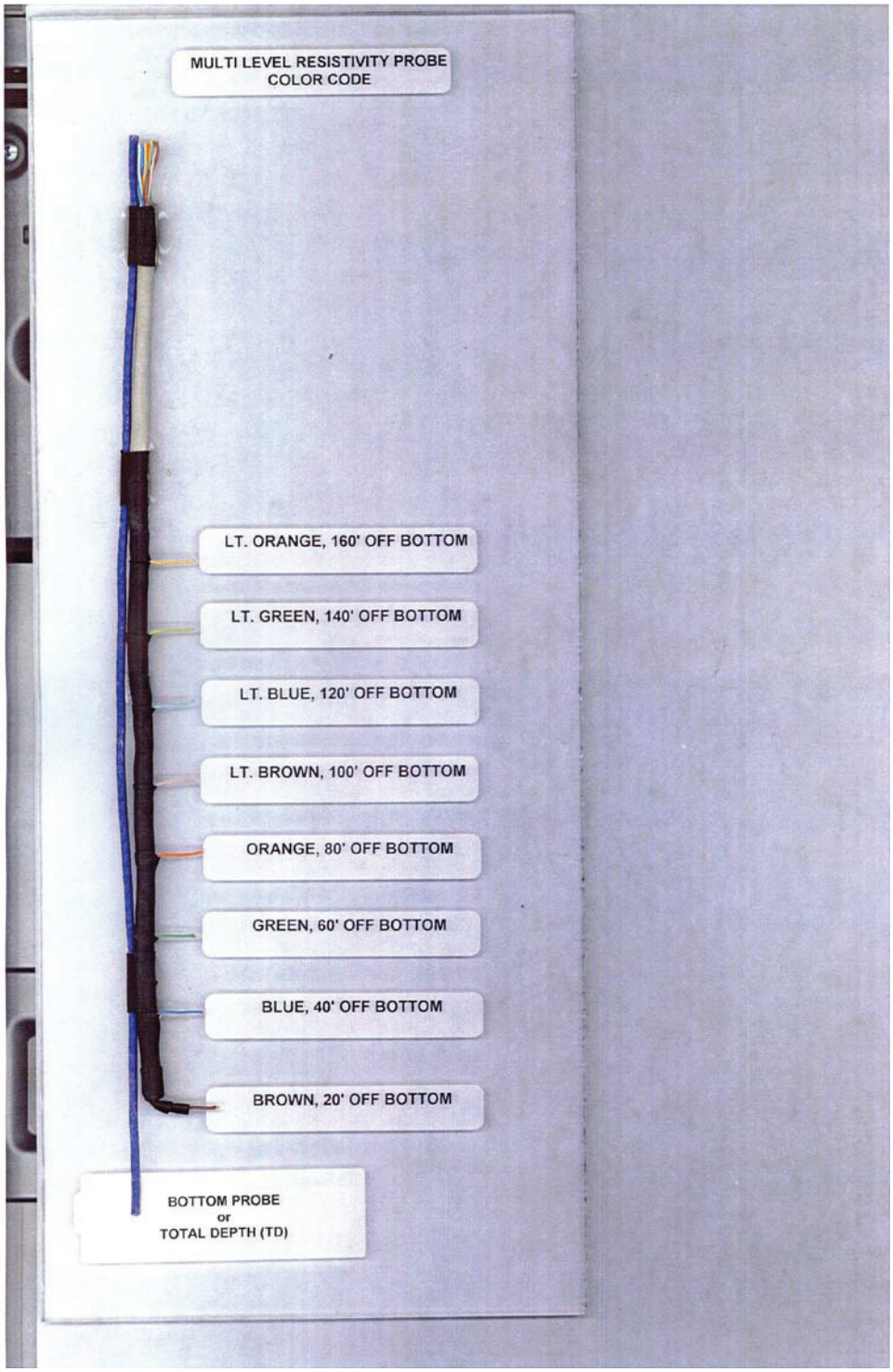

Figure 3-2. Multi-Core Cable with Steel Braid Depth Electrode Example.

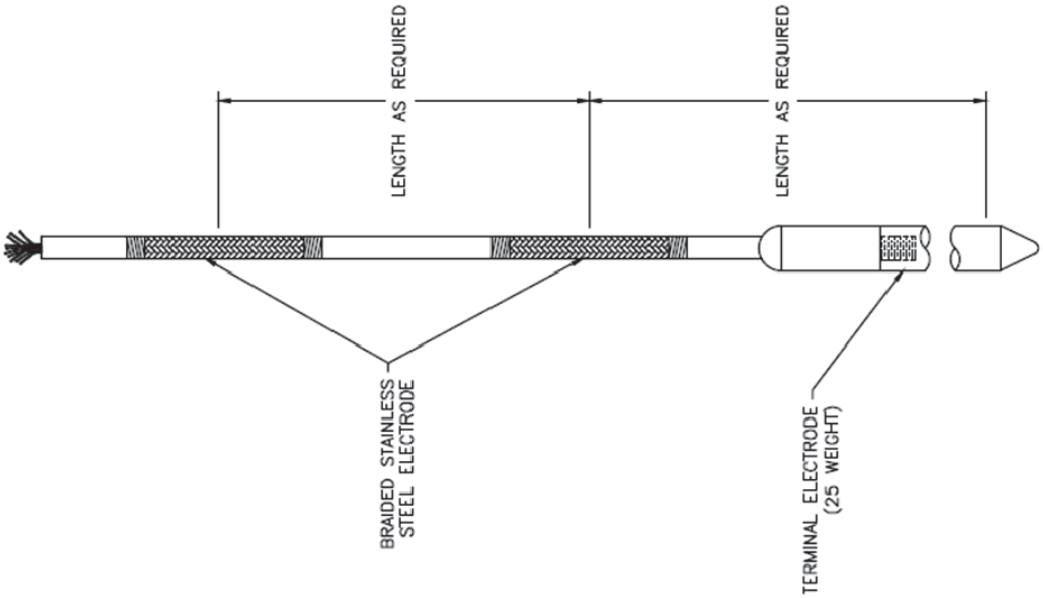

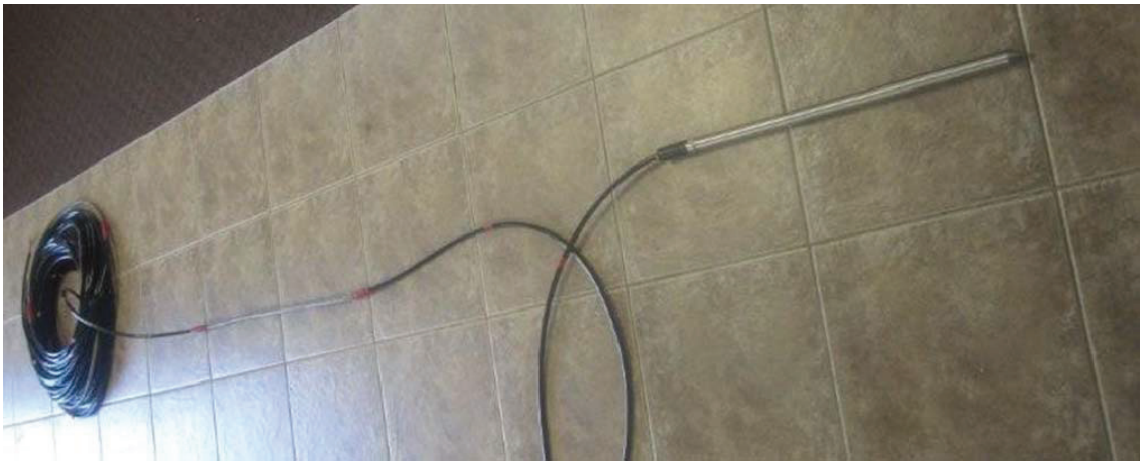

3.2 DATA ACQUISITION WITH DEPTH ELECTRODES

The performance of the different types of electrodes can be explored as shown in Figure 3-4 through output current, repeat error, and reciprocal error. Table 3-6 lists the summary statistic for current transmission from each of the depth electrodes. Using a cut-off value of 240 milliamp (mA) for average current, almost half of the S-SX exposed wire multi-probe electrodes are unusable. All dual-probe and braided wire multi-probe electrodes for S-SX are above the threshold. B farm electrodes are all below the threshold. All but one from both UPR-81 and UPR-86 are usable.

Table 3-6 shows the summary statistics for the repeat error, as calculated internally by the resistivity meter. The repeat error is the standard error of the mean calculated from a set of repeat measurements of voltage, expressed as a percentage. Using a cut-off value of 1.2 percent, only three of the 14 electrodes for the exposed wire multi-probe array are suitable for use, one of the dual-probe electrodes is suitable, and six of seven braided wire multi-probe electrodes are useable. All of B farm are essentially unusable, three of four UPR-81 are usable, and all of UPR-86 are usable.

Table 3-6 listing the summary statistics for the reciprocal error. The reciprocal error represents the difference in voltage measurement between an electrode pair when they switch roles as transmitter and receiver. Two columns are listed for the reciprocal error, the average reciprocal error and the percentage of data retained for constructing the input file for inverse modeling (after editing), based on a 5 percent cut-off error. Most of the exposed wire multi-probe electrodes in C7737, C7739, and C7741 appear to be under performing with respect to the reciprocal error. The averages are quite high, with only six of 14 having an average less than or equal to 10. In contrast, all of the dual-probe and all but one of the braided multi-probe electrodes have an average less than 10. The averages for UPR-81 are all greater than 10, and the averages for UPR-86 are all less than 10. The averages appear to correlate with the total percentage of data retained for use in the inverse modeling.

A performance measure can be computed for each individual depth electrode by summing the number of times each electrode passes the cut-off measure for the three statistics above. Figure 3-3 shows the performance measure for all of the electrodes, which can take on values of {0, 1, 2, 3}. The electrodes have been sorted from low to high, and it would be reasonable to assess good performance with a 2 or 3, marginal performance with a 1, and poor performance with a 0. It is clear that most of the exposed wire multi-probes electrodes perform marginal to poor, with one performing excellently with a performance measure of 3 (C7739 at 93ft), and four electrodes with a performance measure of 2. Six of the seven braided wire multi-probe electrodes performed excellently, with the exception of C7745 at 153ft.

Table 3-6. Depth Electrode Data from All Projects. (2 Sheets)

Electrode Name	Location	Probe Depths (ft)	Moisture Content (%)	Average Transmitting Current (mA)	Average Repeat Error (as Rx in %)	Average Reciprocal Error (% difference)	Percentage Depth Electrode Data That Fall Below Recip Error Cut-off
C7737	S-SX	60	20	72	1.4	35	22
		80	8	226	1.4	5	83
		100	8	393	1.5	5	86
		120	8	280	1.5	10	67
		140	16	141	1.4	14	44
		159	12	135	1.5	90	6

Table 3-6. Depth Electrode Data from All Projects. (2 Sheets)

Electrode Name	Location	Probe Depths (ft)	Moisture Content (%)	Average Transmitting Current (mA)	Average Repeat Error (as Rx in %)	Average Reciprocal Error (% difference)	Percentage Depth Electrode Data That Fall Below Recip Error Cut-off
C7739	S-SX	93	10	284	1.2	6	85
		113	15	282	1.4	8	76
		133	8	513	1.4	4	86
		152	22	124	1.5	16	60
C7741	S-SX	33	9	509	0.9	135	1
		53	4	191	1.1	25	28
		133	20	426	1.4	47	22
		152	15	499	1.4	100	3
C7743	S-SX	36	13	524	1.1	4	90
		97	20	493	1.3	4	88
C7745	S-SX	10	4	355	1.2	5	84
		31	8	433	1.1	4	91
		51	9	466	1.1	4	89
		71	13	474	1.1	5	88
		91	15	487	1.1	5	90
		111	13	489	1.1	5	86
		153	25	515	1.4	100	2
C5161	B-Farm	55	not collected	156	7.2	not collected	n/a
C5165	B-Farm	55	6	195	7.3	not collected	n/a
C5177	B-Farm	35	6	193	8.5	not collected	n/a
C5179	B-Farm	35	8	207	8.4	not collected	n/a
C6395	UPR-81	50	9	246	1.8	153	3
		146	7	140	0.9	583	20
C6399	UPR-81	50	6	246	0.9	231	35
		215	5	243	0.9	143	1
C5943	UPR-86	90	3	428	0.2	3	96
C5947	UPR-86	150	3	15	0.2	8	47
C5957	UPR-86	143	3	493	0.3	3	96
C5959	UPR-86	95	7	237	0.3	3	98
C5963	UPR-86	95	7	373	0.3	3	96

Figure 3-3. Performance Measure for Each of the Depth Electrodes.

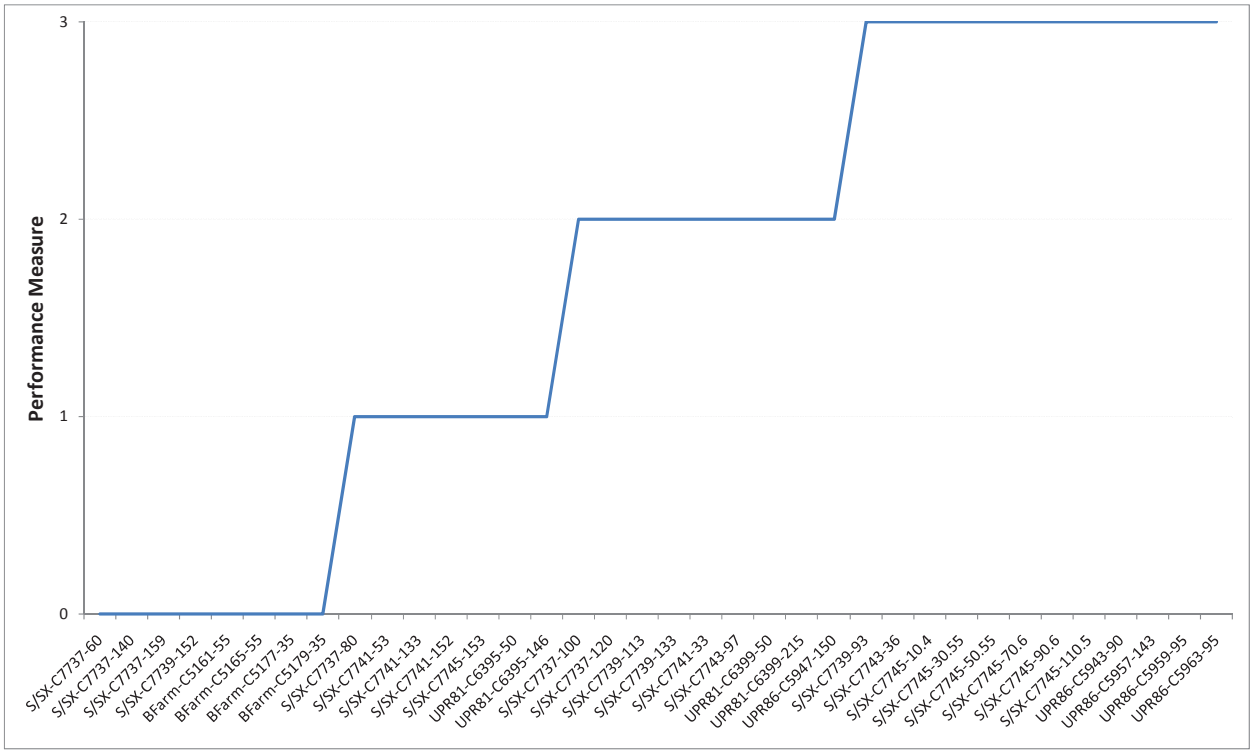

Note: Performance of 0 = Poor; Performance of 1 = Marginal; and performance of 2 or 3 = Good.

Table 3-7. Depth Electrode Time Differential from All Projects.

Electrode Name	Location	Probe Installation	Resistivity Survey	Time Difference (months)	Method of Completion	Surrounding Media
C7737	S-SX	2/2010	6/2010	4	No Water	Sand with Salt
C7739	S-SX	2/2010	6/2010	4	No Water	Sand with Salt
C7741	S-SX	2/2010	6/2010	4	No Water	Sand with Salt
C7743	S-SX	3/2010	6/2010	3	Salt Water	Sand
C7745	S-SX	3/2010	6/2010	3	Tap Water	Diatomaceous Earth
C5161	B-Farm	12/1/2006	1/2007	1	Salt Water	Sand
C5165	B-Farm	12/1/2006	1/2007	1	Salt Water	Sand
C5177	B-Farm	12/1/2006	1/2007	1	Salt Water	Sand
C5179	B-Farm	12/1/2006	1/2007	1	Salt Water	Sand
C6395	UPR-81	5/1/2008	11/2008	6	Salt Water	Sand

Table 3-7. Depth Electrode Time Differential from All Projects.

Electrode Name	Location	Probe Installation	Resistivity Survey	Time Difference (months)	Method of Completion	Surrounding Media
C6399	UPR-81	4/1/2008	11/2008	7	Salt Water	Sand
C5943	UPR-86	11/1/2007	3/2010	28	Salt Water	Sand
C5947	UPR-86	11/1/2007	3/2010	28	Salt Water	Sand
C5957	UPR-86	11/1/2007	3/2010	28	Salt Water	Sand
C5959	UPR-86	11/1/2007	3/2010	28	Salt Water	Sand
C5963	UPR-86	11/1/2007	3/2010	28	Salt Water	Sand

To identify the potential causes for the performance, the moisture content as measured from neutron probe geophysical logging at the exact depth of placement, time difference between depth electrode installation and usage, and methods of completion are presented in Tables 3-6 and 3-7, respectively. Surprisingly, there are no correlations between electrode performance and antecedent moisture content. There does appear to be a correlation between time difference and performance, where longer times between installation and usage caused better performance. Exceptions were for the S/SX electrodes C7743 and C7745 that had a smaller time differential and great performance. The completion method also had a significant influence, where moisture added to the soil around the electrode caused a higher performance. The exception is for B farm data, where water was added but the electrodes performed poorly. Yet these electrodes were used within a month of installation. In summary, it appears that moisture is needed around the electrode and a nominal time difference between installation and usage is preferred (three to four months).

3.3 CHRONOAMPEROMETRY

As the final means of evaluating the performance of the different electrodes at the S-SX tank farm area, an investigation into the temporal behavior of the electrodes was conducted. In general, electrodes installed in areas of limited moisture may behave erratically due to the exhaustion of the surrounding moisture from excessive electrical current. Initially, upon current injection they appear to behave normally, but as time progresses and moisture is broken down through electrolysis, the amount of current the electrode can carry diminishes. The phenomenon is called over-driving the electrode, whereby the resistivity instrument is trying to force more current through the electrode than the than the electrode and surrounding earth will support before electrolysis removes too much moisture and raises the contact resistance to a level that produces unacceptable data.

The ideal response of an electrode over time would be a constant electrical current output from a constant applied voltage from the transmitter. Fortunately, the temporal sequence of transmission data can be obtained from the S-SX survey and plotted to observe the behavior. It

should be kept in mind that the SuperSting R8® has an automatic function to briefly transmit current in order to determine the electrode's capability to transmit current and to set the SuperSting R8 transmitter gain level. If the electrode fails the test, then the instrument lowers the current level and tries again. It will continue to lower the current until a level is reached that it believes the electrode will support. Desirable characteristics for an electrode are relatively high current (depending on the instrument) and relatively low voltage. The combination of the two parameters constitutes the electrode-to-ground contact resistance. Anytime the transmitted current in milliamps is higher than the transmitted voltage in volts, that generally signifies a stable electrode.

Figure 3-4 shows an example of a stable electrode, where data were taken from the braided multi-probe electrode at a depth of 50.5 ft. The abscissa represents the time of day on June 20, 2010 for the measurements. The electrical current is stable over the 10-minute sequence and is higher than the voltage. Figure 3-5, on the other hand, shows an unstable electrode. After the initial transmission, the current was raised (automatically by the instrument) to 252 mA at 304 volts. At that level, the electrode was over-driven and subsequent currents monotonically declined to less than 50 mA. Voltage quickly rose to the maximum output of the instrument at 400 volts and maintained this level. This electrode should only be operated at less than 100 mA to minimize long-term damage to the electrode.

The ratio of voltage to current (in ohms) is presented in Figure 3-6 for all of the electrodes of the S-SX tank farm. The abscissa for Figure 3-6 represents a generic time series count to allow the time series from each electrode to be presented together. The number of measurements occurred over a 10-20 minute interval, with each electrode performing up to 225 "shots." The figure clearly separates the poor performing electrodes from the good performing electrodes, with a few intermediate electrodes labeled marginal. There appears to be a great deal of overlap between the performance in Figure 3-6 with that of Figure 3-2. For example, C7737 at 80 ft shows marginal performance in both figures. It should be noted, however, that good transmission characteristics does not necessarily guarantee good receiver characteristics, as measured through the repeat error and reciprocal error.

® SuperSting R8 is a registered trademark of Advanced Geosciences, Inc.

Figure 3-4. Temporal Performance of a Stable Electrode.

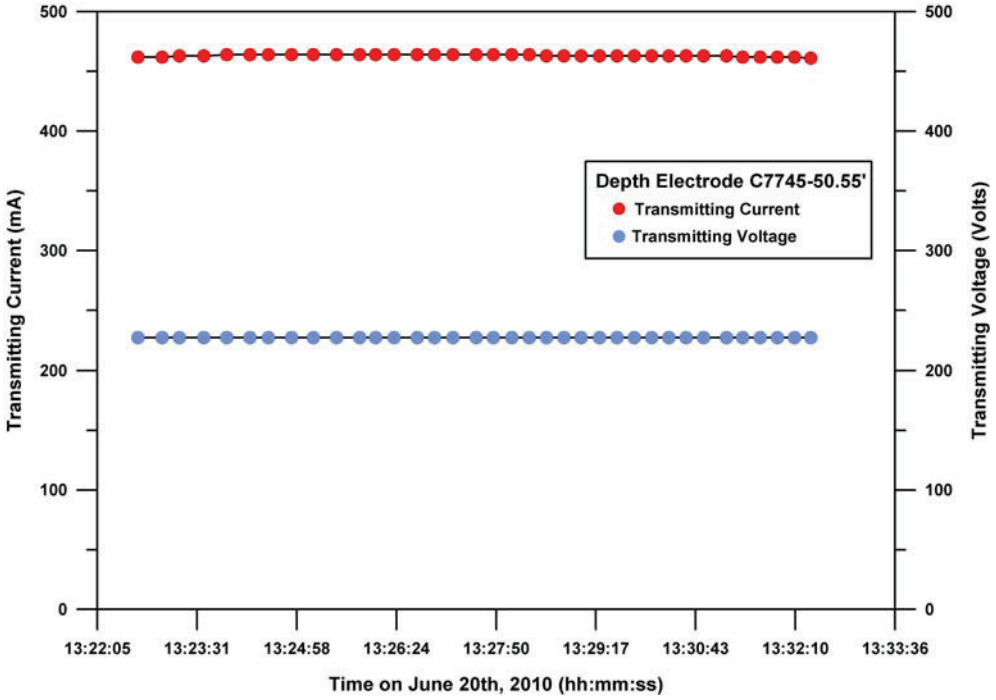

Figure 3-5. Temporal Performance of a Unstable Electrode.

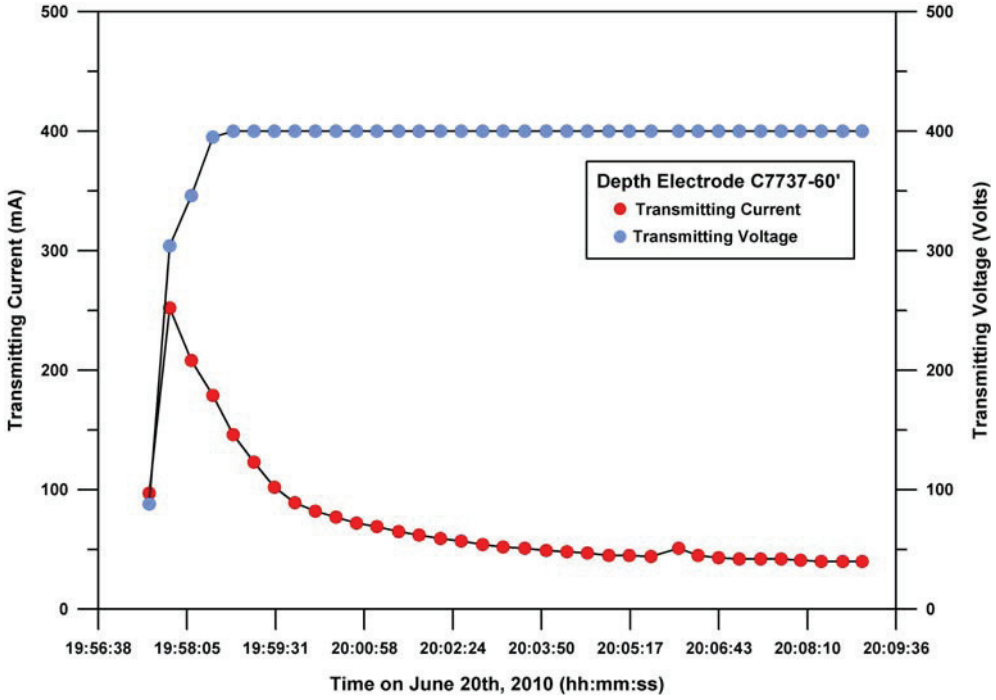

Figure 3-6. Temporal Performance of a Unstable Electrode.

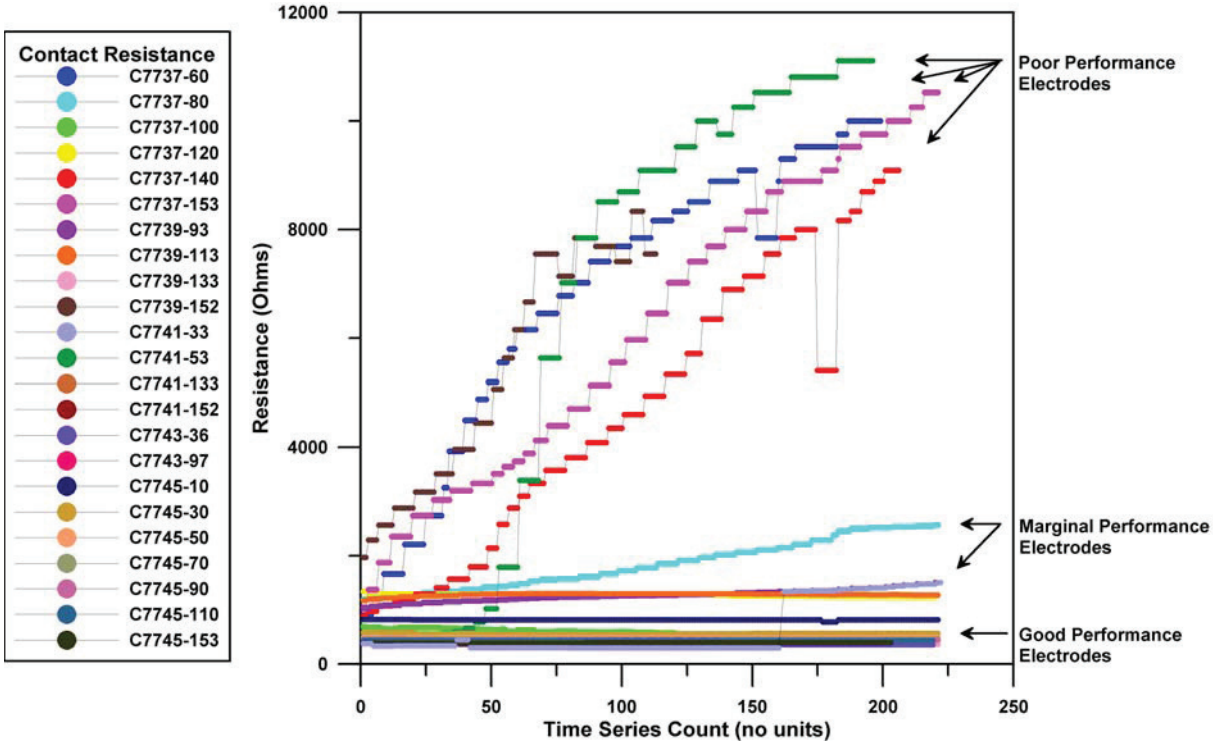

4.0 PRELIMINARY MODELING RESULTS

Upon completion of data filtering, measured apparent resistivity data from the S-SX tank farm site were inverse modeled using the RES3DINVx64 software package. For specific details of the SGE resistivity method and theoretical basis applied to inverse modeling, the reader is referred to discussions provided in RPP-34690.

To accomplish the 3D inversion, every surface, depth, and long electrode was geo-referenced (using the Washington State Plane – Meters coordinate system) to allow absolute placement of an electrode within the inversion algorithm. The model was then run with a set of input parameters that have been demonstrated to work well in tank farm environments. After inversion, the final 3D inversion results were interpolated to a regular grid and visualized using the Rock Works™ visualization software package and Surfer® surface contouring package. The visualization allows discrimination of low resistivity targets that could be associated with increased moisture, increased ionic strength of the pore water, infrastructure, or a combination of these items. It is anticipated that mineralogy and porosity would have minimal effects on the resistivity outcome.

4.1 INVERSE MODELING RESULTS

To create the datasets for inversion, two types of data reduction occurred between the data acquisition and final plotting phases. First, data quality was inspected to eliminate unacceptable data that may have resulted from instrumentation error, electrical interference, or high data misfit with respect to neighboring points. The process of removing spurious data points is referred to as editing and is performed prior to the first inversion run. Second, data were filtered after each inverse model was completed to remove data points that contributed to a high model RMS error. This process is referred to as a filter run, and the objective of a filter run was to get the final RMS to an acceptable level. Each model was assigned a model number which designated a specific data set or set of modeling parameters and each filter run was assigned a number. An example label for a model with two filter runs is "Model_001_ii." At most, two filter runs were conducted on the models, with some models requiring no filter runs.

4.1.1 Surface to Surface Only

The initial model, Model 001, focused on the 3D data set using only the highest quality measured STS resistivity data, with no depth or long electrodes. A high quality dataset for inversion was obtained by removing those data with repeat errors greater than 2 percent and reciprocal errors greater than 5 percent. After noisy data removal, 26,446 data values remained for inclusion in the model. Two filter runs were completed on Model 001 with a final data count of 21,635 for the last filter run.

A collection of 3D views, rendered from RES3DINVx64 results, are provided in Figure 4-1. The results from the last filter run (Model 001_ii) are shown below. These plots show a 3D

™ Rock Works is a trademark of Rockware, Inc
® Surfer is a registered trademark of Golden Software, Inc.

distribution of resistivity values where the resistivity colors are transparent, such that values at multiple resistivity isopleths can be viewed. Specifically, the plots show two resistivity ranges, in log scale, of -0.5 to 0.4 Ohm-meters in red, and 0.4 to 0.7 Ohm-meters in green. The plan view Figure 4-1 (A) represents a cumulative spatial distribution of inverted resistivity subsurface conditions, as seen from above. Plot Figure 4-1 (B) presents an oblique view of the model and Figure 4-1 (C) shows a view looking east for the same model.

Figure 4-1. Distribution of Calculated Resistivity for Inverse Model 001_ii.

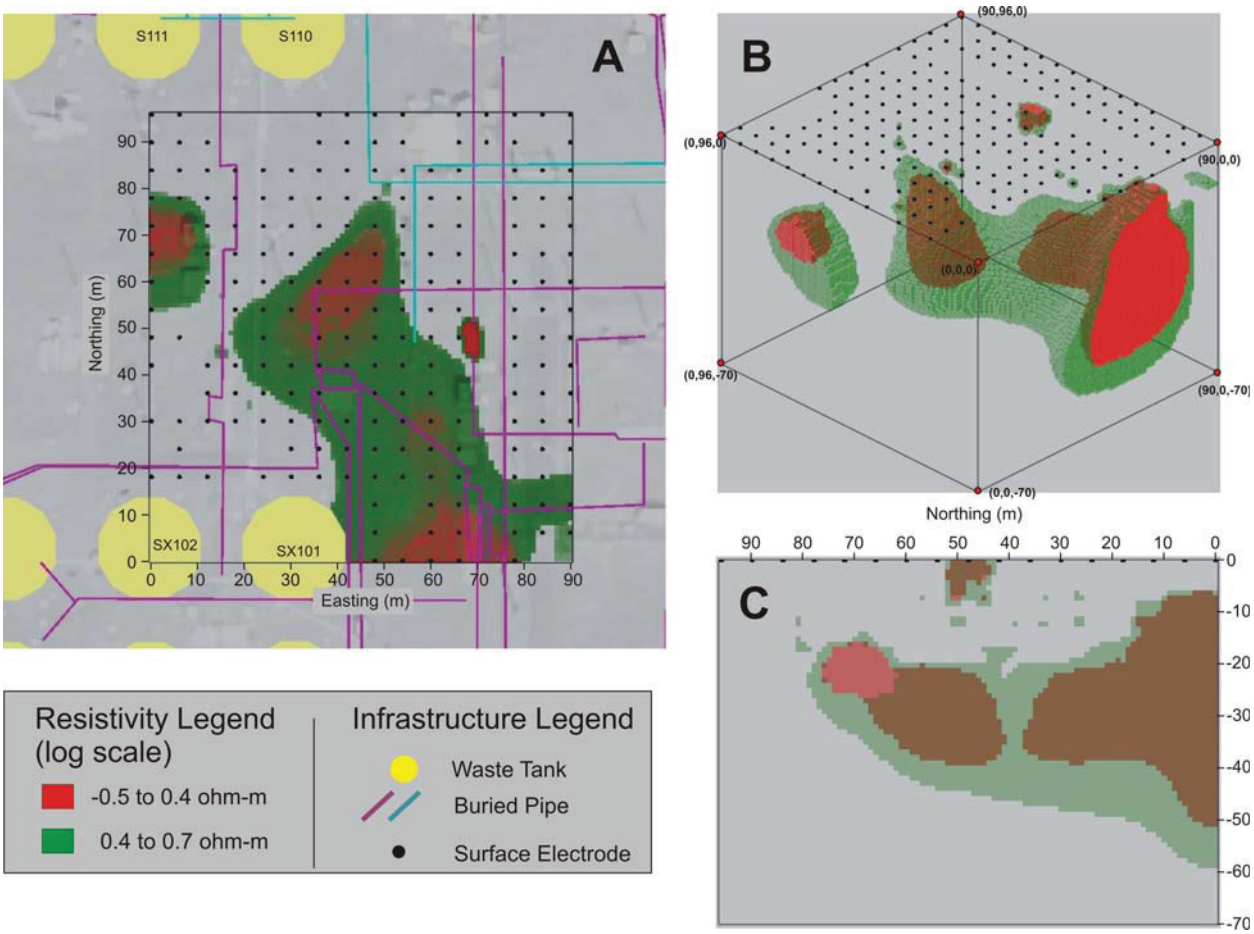

(A) Plan View, (B) Oblique View, looking Northeast, (C) Side View, looking East,

In general, the model shows a low resistivity target in the middle of the domain that extends to the south-southeast. The view looking east, essentially showing a profile through the domain, shows that the low resistivity target is not at the surface, but ranges from about 20 to 40 meters bgs. The depth of the target would suggest that infrastructure is only playing a minor role in creating the target, except along the southern border. However, the resistivity values appear quite low with the red solid rendering representing up to 2.5 Ohm-meters. An increase in moisture could be the main contributor to the low-resistivity target, and Figure 4-2 shows moisture values digitized from neutron geophysical logging data at C7739. There is an increase

in moisture starting around 25 meters depth, and the figure is highlighted to show the depth of the resistivity target from 20 to 40 meters.

Figure 4-2. Neutron Logging Moisture Data from C7739.

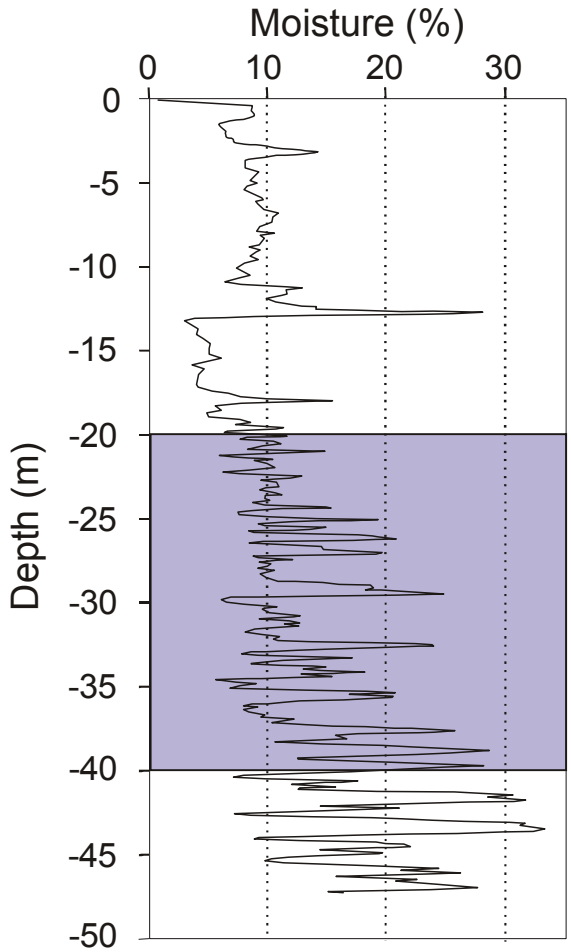

Plan view horizontal depth slices for Model 001_ii, shown in Figure 4-3, present modeling results at increasing depths in meters bgs. The slices are meant to provide more detail regarding the distribution of electrical resistivity in the subsurface. The upper most layer at 6 meters does show some low resistivity features that track with the infrastructure. By 16 meters however, the influence of the infrastructure on the low-resistivity target is absent.

Figure 4-3. Plan View Depth Slices of Distribution of Calculated Resistivity for Inverse Model 001_ii.

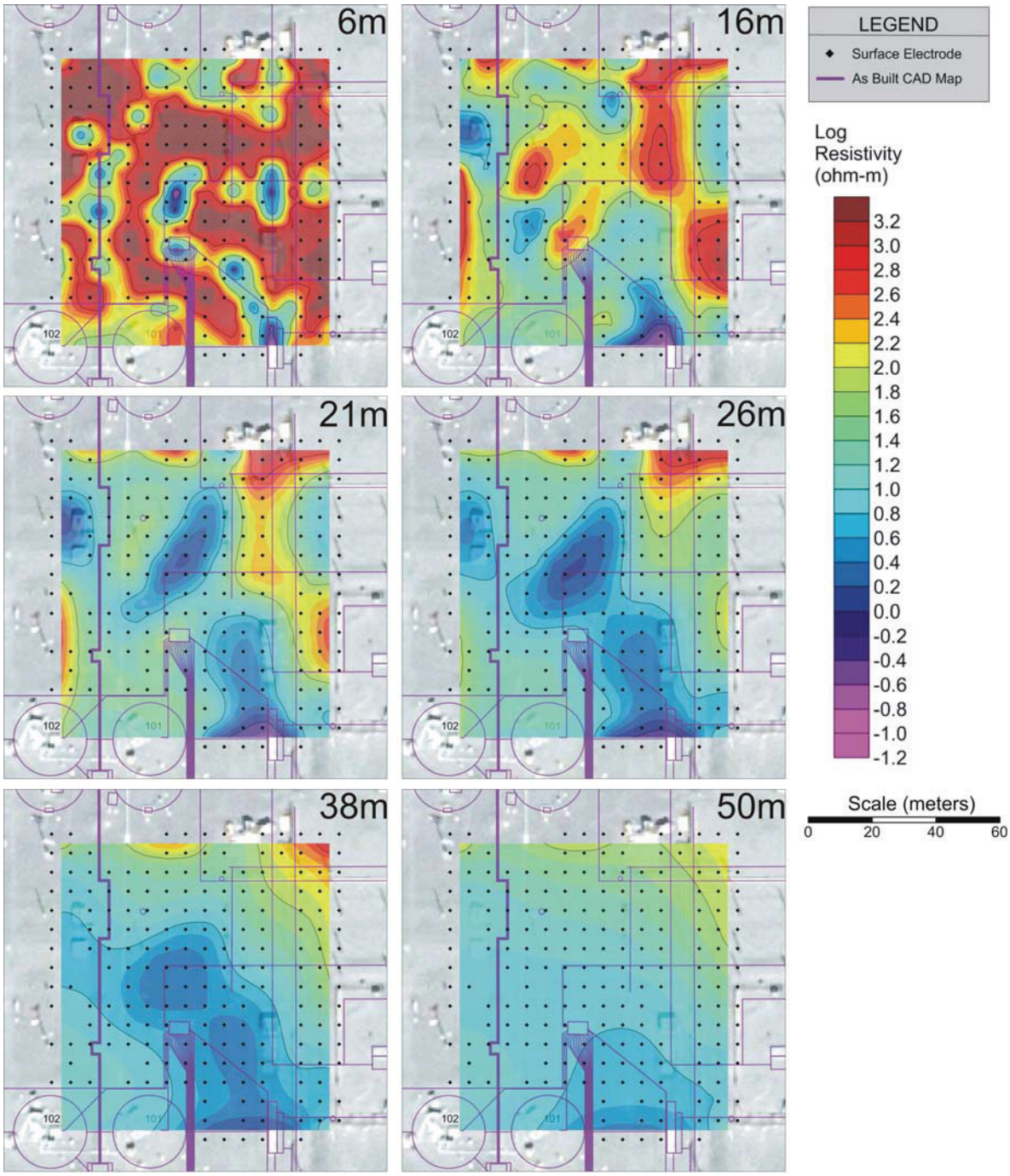

4.1.2 Surface-to-Surface with Depth Electrodes

Previous inverse modeling performed at the UPR-81 and UPR-86 site showed that those models with depth electrodes had better vertical resolution compared to STS data alone. It was determined that a dramatic improvement could be achieved with even a small quantity of depth electrode data. For the UPR-81 site, only two depth electrodes were used. For the UPR-86 site, there were four available depth electrodes. For the S-SX, the number of usable electrodes increased to 13 (of an available 24 in S-SX tank farm). Unfortunately, 11 of the 24 available electrodes were unusable based on the quality of data from the electrode.

Model 024 focused on the 3D data set using STS and depth electrode resistivity data. This model used the identical STS dataset modeled in Model 001_ii, but also included additional data from the depth electrodes. After noisy data removal, 24,078 data values remained for inclusion in the model, with 10.1 percent of the data involving depth electrodes as DTS. A single filter run was completed for Model 024 (named Model 024_i), with a final data count of 23,009.

A collection of 3D views from Model 024_i, rendered from RES3DINVx64 results, are provided in Figure 4-4. These plots show a 3D distribution of resistivity values where the resistivity colors are transparent such that values at multiple resistivity isopleths can be viewed. Specifically, the plots show two resistivity ranges, in log scale, of -0.5 to 0.4 Ohm-meters in red, and 0.4 to 0.7 Ohm-meters in green. The plan view Figure 4-4 (A) represents a cumulative spatial distribution of inverted resistivity subsurface conditions, as seen from above. Plot Figure 4-4 (B) presents an oblique view of the model, and Figure 4-4 (C) shows a view looking east for the same model.

The results of the inversion with depth electrodes show a significantly smaller set of targets compared to the STS data alone. The scattering of the remaining targets, mostly along the perimeter of the model, are reminiscent of noise in the inversion and may not actually represent much in the way of subsurface contamination. The exception is the large low-resistivity target on the southern extent of the domain, which may be the results of infrastructure or increased moisture. The depth electrodes, located deeply beneath the infrastructure, likely provided the additional sensitivity necessary to properly resolve subsurface features compared to the Model 001 series.

Figure 4-4. Distribution of Calculated Resistivity for Inverse Model 024_i.

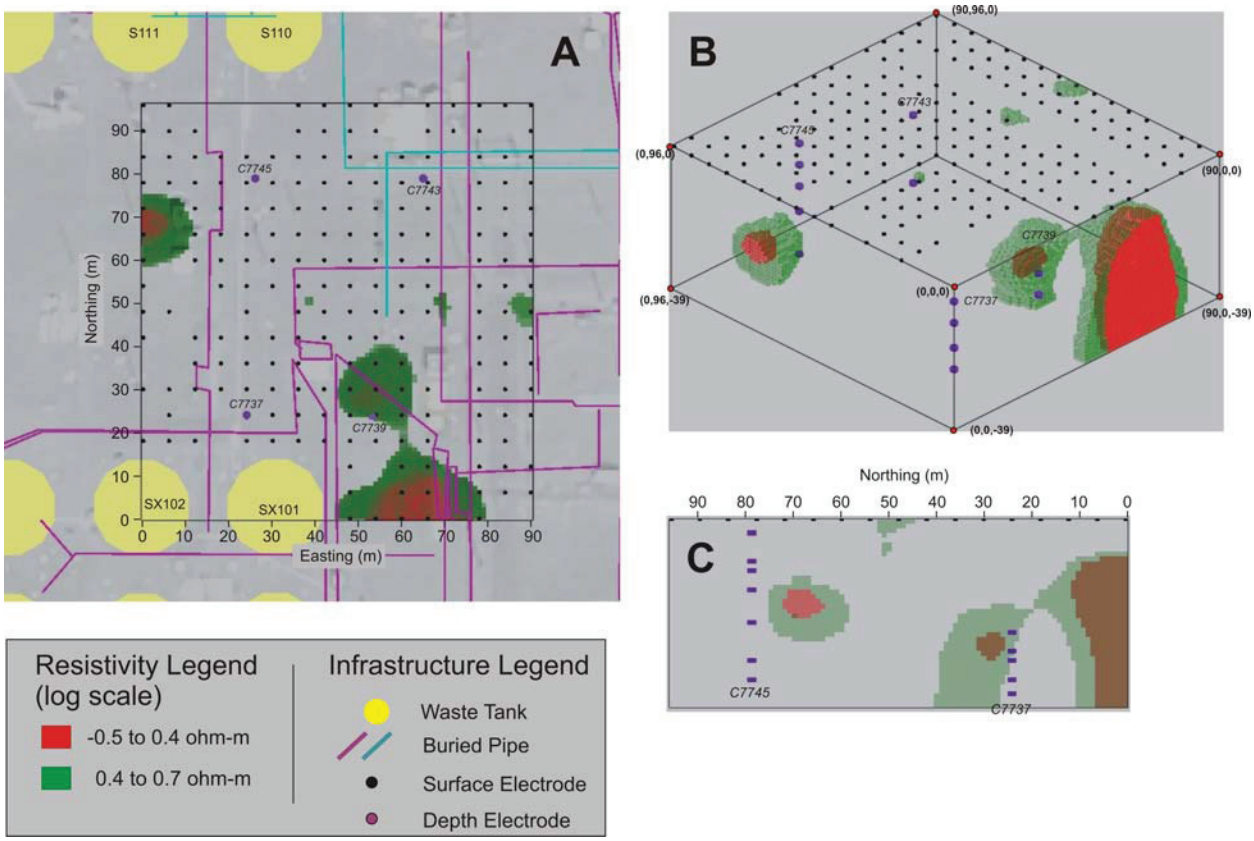

(A) Plan View, (B) Oblique View, looking Northeast, (C) Side View, looking East

Plan view horizontal depth slices for Model 024_i, shown in Figure 4-5, presents modeling results at multiple depths in meters bgs.

Figure 4-5. Plan View Depth Slices of Distribution of Calculated Resistivity for Inverse Model 024_i.

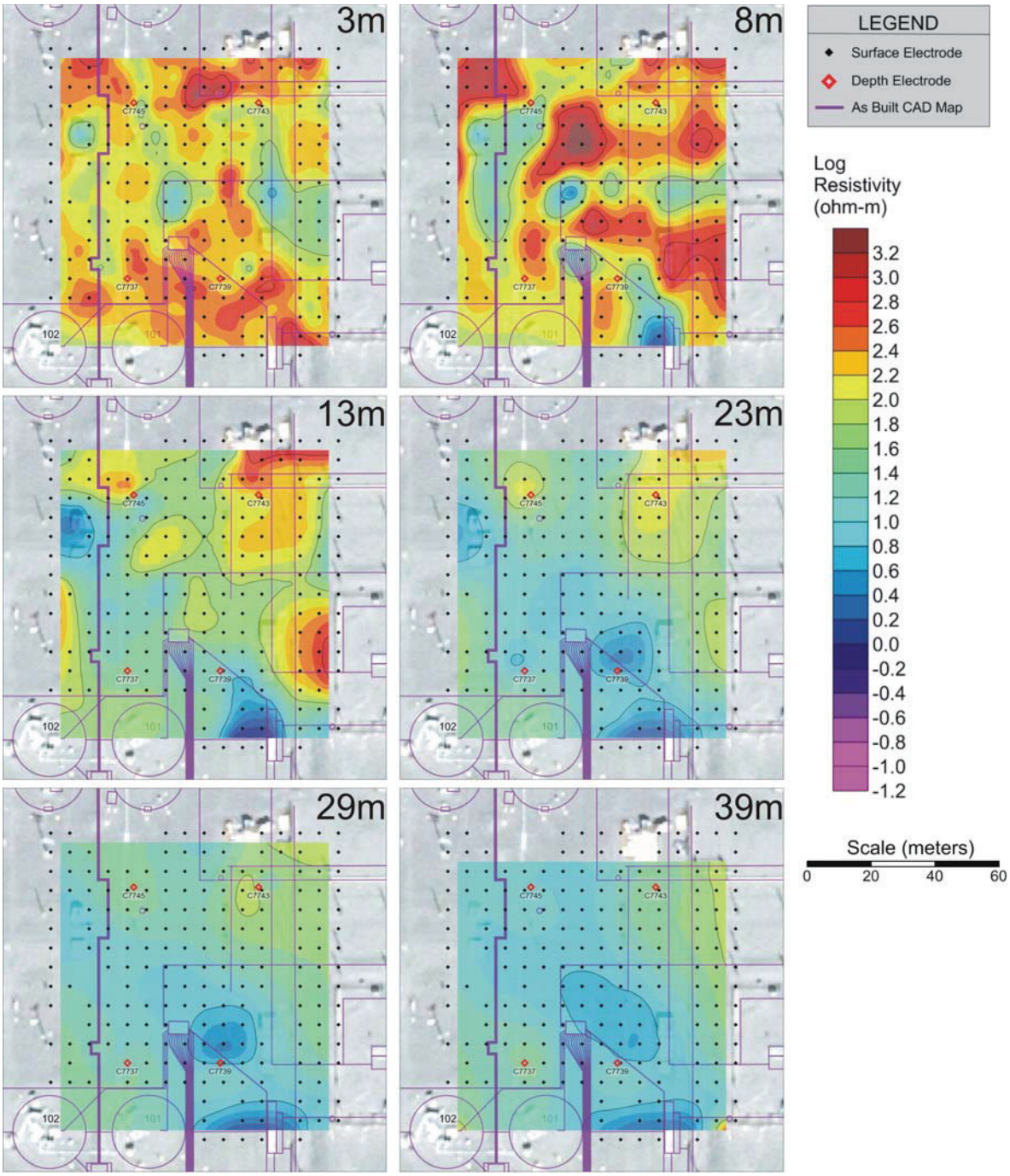

4.1.3 Surface, Depth, and Long Electrodes

The last set of models included using the wells as long electrodes in the inversion model, along with surface and depth electrodes. The wells were mostly located on the periphery of the domain, with the exception of one well in the center of the domain. The advantage of using the wells as electrodes has been to image plumes in infrastructure rich areas. The disadvantage has been the lack of vertical resolution and low spatial density providing low lateral resolution. Previous inversion modeling software was unable to produce acceptable model results using combined point source (surface and depth electrodes) and linear source (wells) electrodes. However, HGI's continued work with Geotomo, Inc had produced an updated version of RES3DINVx64 that solves the combined model more accurately. It was hoped that the wells coupled with depth and surface electrodes would provide additional resolution while effectively seeing through the near-surface infrastructure.

Model 026 focused on the 3D data set using STS, DTS, depth-to-well, and well-to-surface (WTS). After noisy data removal, 29,637 data values remained for inclusion in the model. A single filter run was completed for Model 026 (named Model 026_i), with a final data count of 28,811.

A collection of 3D views from Model 026_i, rendered from RES3DINVx64 results, are provided in Figure 4-6. These plots show a 3D distribution of resistivity values where the resistivity colors are transparent such that values at multiple resistivity isopleths can be viewed. Specifically, the plots show two resistivity ranges, in log scale, of -0.5 to 0.4 Ohm-meters in red, and 0.4 to 0.7 Ohm-meters in green. The plan view Figure 4-6 (A) represents a cumulative spatial distribution of inverted resistivity subsurface conditions, as seen from above. Plot Figure 4-6 (B) presents an oblique view of the model, and Figure 4-6 (C) shows a view looking east for the same model.

The results of Model 026_i shows a low resistivity target smaller than Model 001_ii, but larger than Model 024_i. Figure 4-6 shows low resistivity values in the center of the domain, extending towards the southeast. The addition of the wells for Model 026 essentially added an extra target that was absent in Model 024. The confidence in this target is low, given that Model 026 is the first model to use all types of available electrodes in a single inversion run and sufficient testing has not yet been completed to fully understand the combined effects from the different types of electrodes. Further testing is needed to ensure that the measured resistivity data can be combined in the manner conducted for Model 026.

Figure 4-6. Distribution of Calculated Resistivity for Inverse Model 026_i.

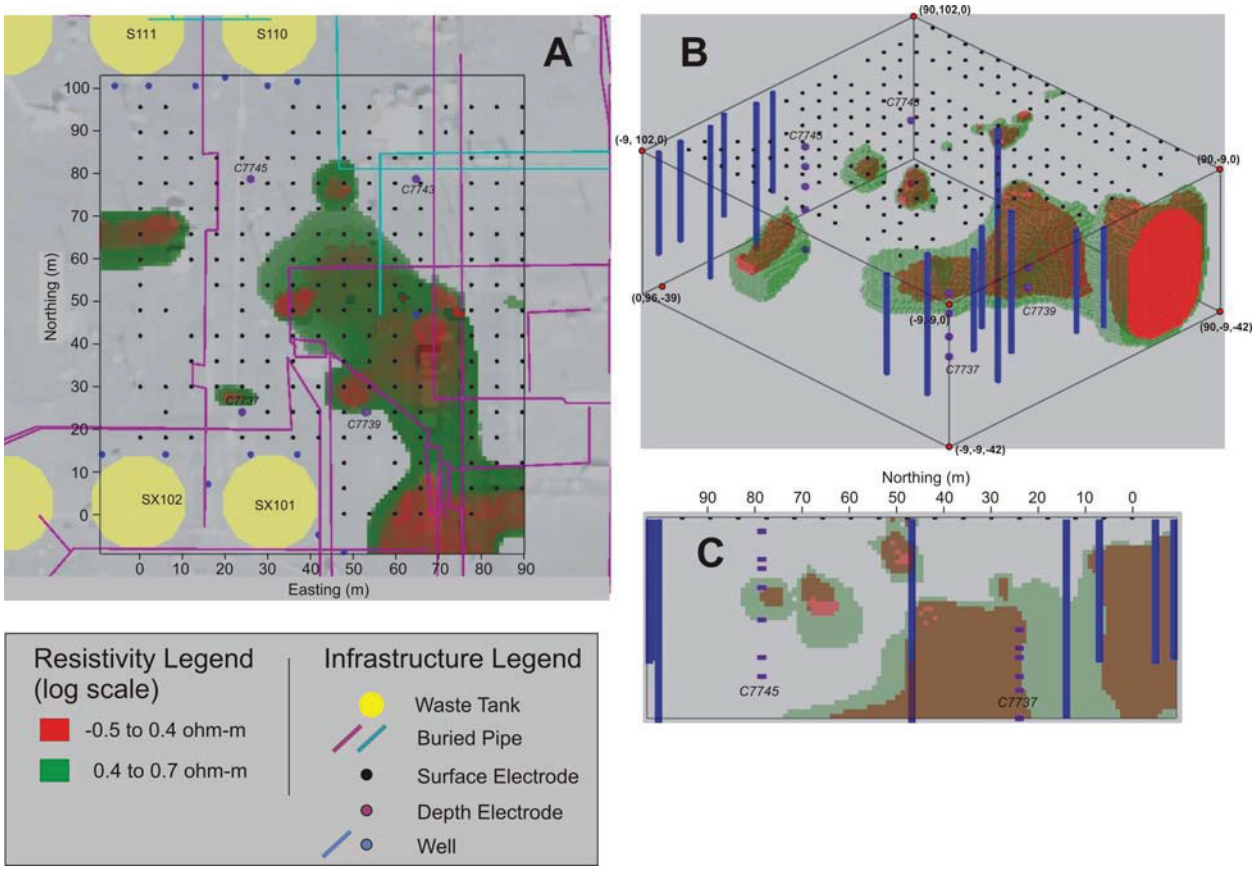

(A) Plan View, (B) Oblique View, looking Northeast, (C) Side View, looking East

Plan view horizontal depth slices for Model 026_i, shown in Figure 4-7, presents modeling results at multiple depths in meters bgs.

Figure 4-7. Plan View Depth Slices of Distribution of Calculated Resistivity for Inverse Model 026_i.

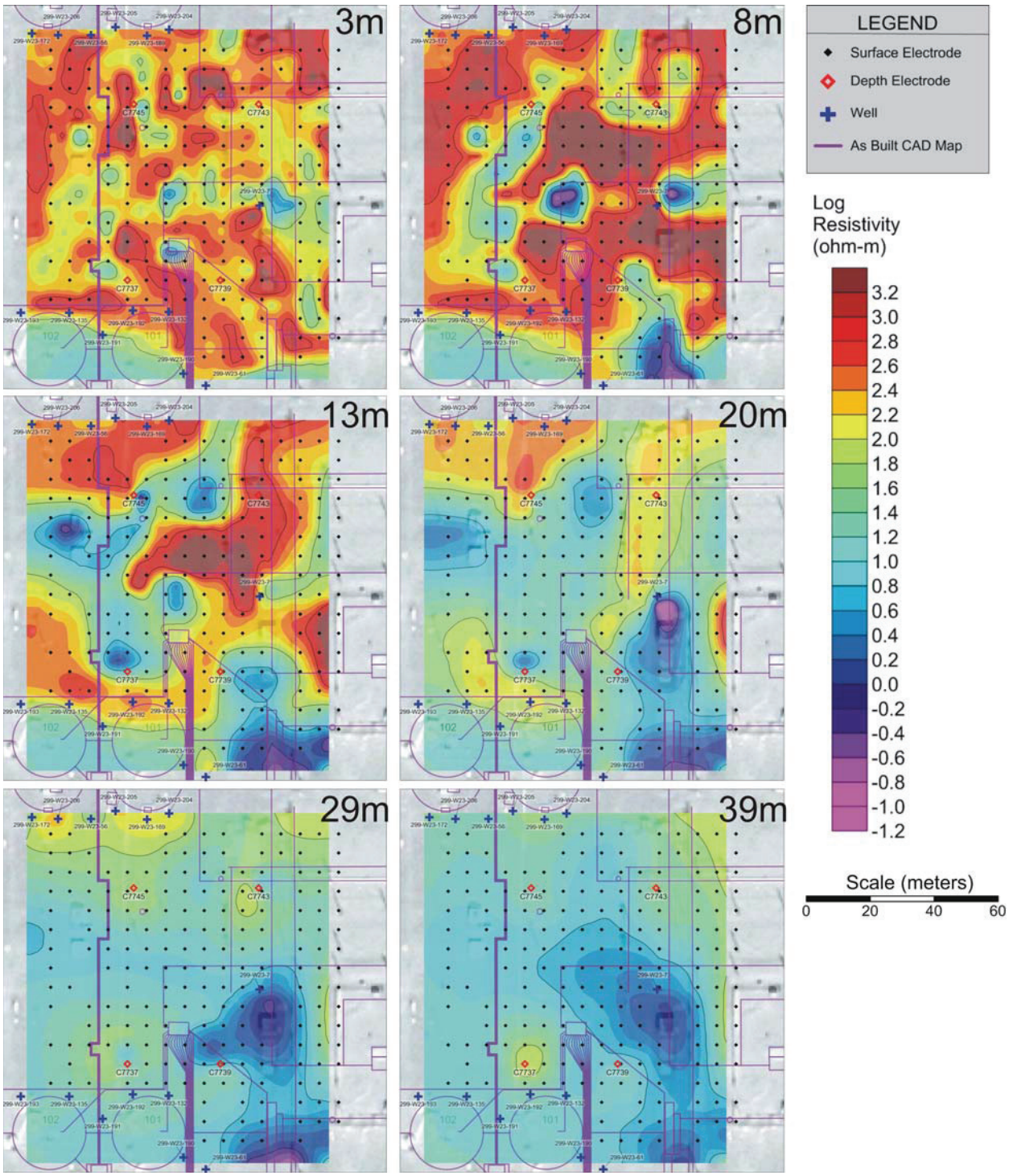

4.2 MODELING PERFORMANCE

Final models for presentation were chosen based on overall performance and quality of the inversions. A means of assessing the performance of an inversion model was to evaluate the convergence and final model error. Convergence curves present changes in the RMS error versus inversion iteration number. Convergence curves for the final models, Model 001, Model 024, and Model 026, are provided in Figures 4-8 through 4-10, respectively.

The RMS error value is an indicator of goodness of fit between the measured data and corresponding calculated values that are provided by RES3DINVx64. It is generally expected that the RMS error should decrease with successive iterations. A deviation from this expected behavior may indicate that the inversion process has become unstable and that isolated high error readings are dominating the model. Additionally, it is normal to see a convergence curve that is not monotonically decreasing for subsequent iterations. Evaluation of the model stability takes the entire trend into consideration.

From a model convergence perspective, all three models were acceptable, but Models 001 and 024 (using only surface electrode data) appear to have produced a more stable solution based on the shape of the resulting convergence curves.

Figure 4-8. Model 001 Convergence Curve.

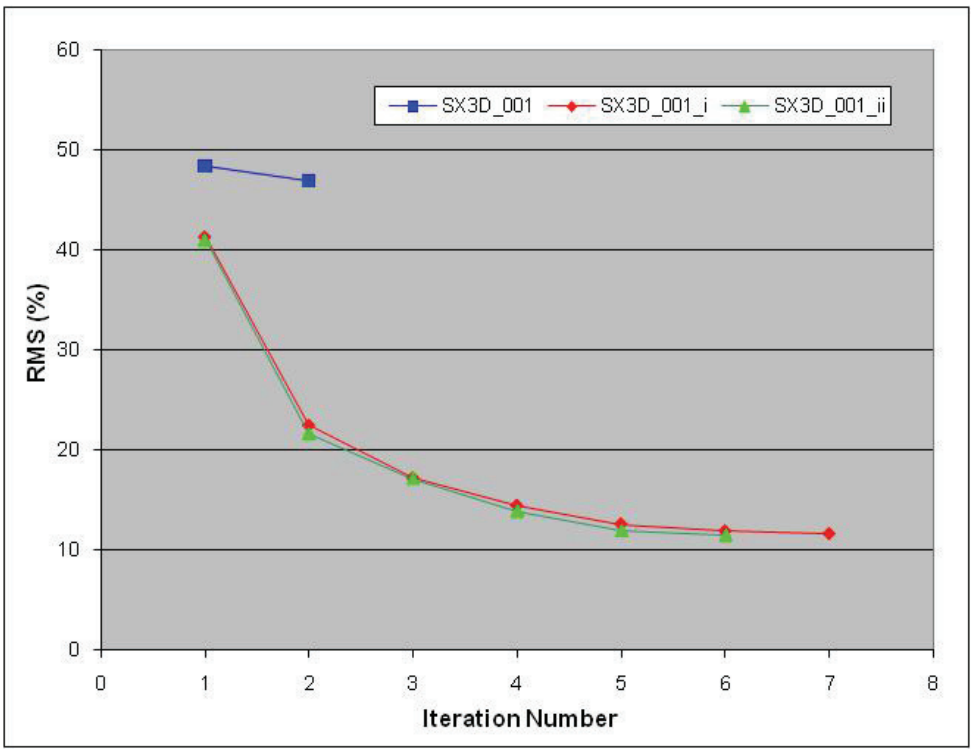

Figure 4-9. Model 024 Convergence Curve.

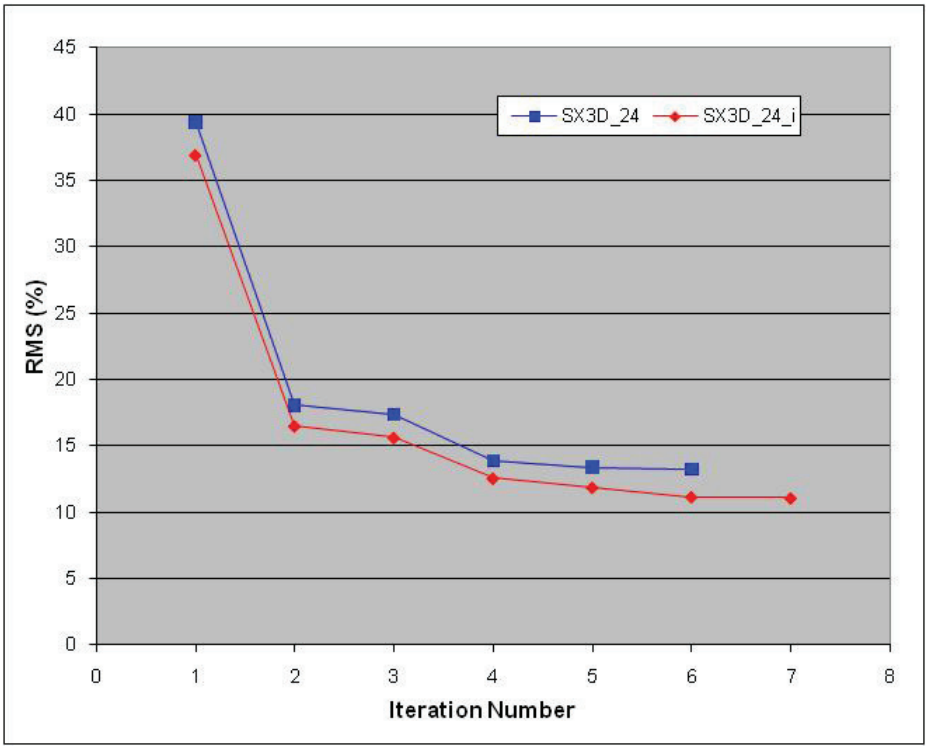

Figure 4-10. Model 026 Convergence Curve.

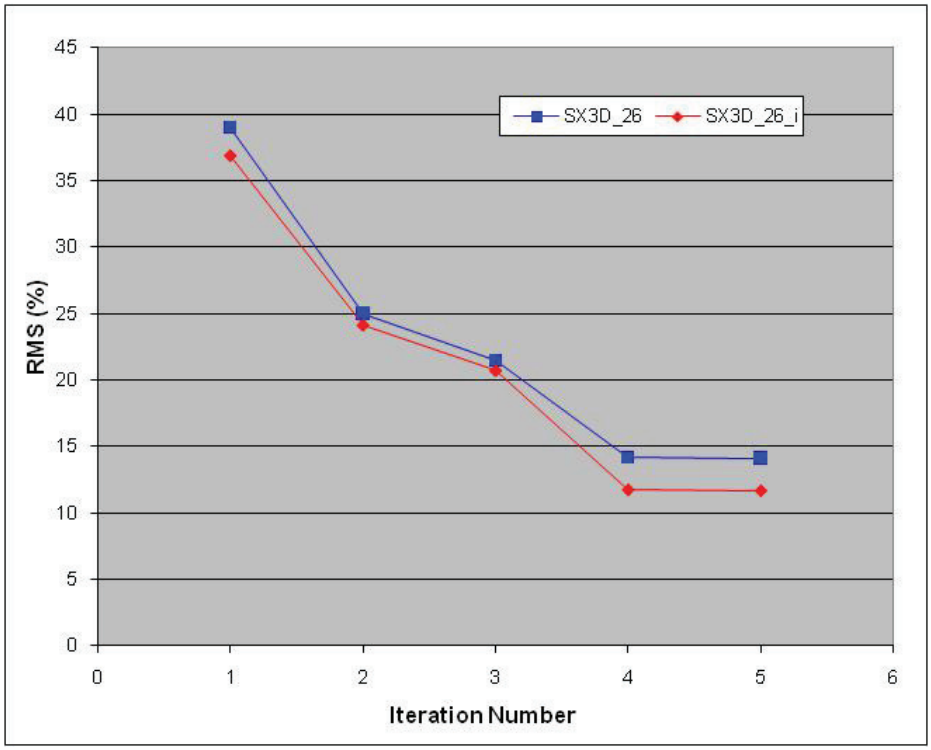

Table 4-1 presents a summary of the data quantity associated with each inversion model and specific electrode set that makes up the dataset.

Table 4-1. Inverse Modeling Convergence and Error Statistics.

	Model 001_ii	Model 024_i	Model 026_i
No. Data Points	26,446	24,078	29,637
No. Data Points after filter	21,636	23,009	28,811
% Data Remaining after filter	81.8	95.5	97.2
RMS Error (%)	11.5	11.89	11.7

5.0 CONCLUSIONS AND RECOMMENDATIONS

The primary objective of the S-SX tank farm survey was two-fold: (1) to map low-resistivity anomalies that can be evaluated as areas of contamination from past leaks and spills, and potentially guide any direct sampling and analysis activities, and (2) to evaluate the performance of depth electrodes in the tank farm relative to past performance in order to understand the effects of different electrode types and completion methods. In order to meet these objectives, electrical resistivity data were acquired with a high-resolution 3D data acquisition method using surface and depth electrodes, and wells as long electrodes. Since it is well known that a substantial amount of metallic infrastructure exists in and around the tank farm, the survey design for electrode placement incorporated existing engineering drawings to identify preferential locations for the electrodes in areas away from the infrastructure where possible.

5.1 DEPTH ELECTRODE ANALYSIS

The following conclusions were derived from the results of a statistical evaluation of the depth electrodes from B farm, UPR-81, UPR-86, and S-SX tank farms:

- **Electrode Design:** The depth electrode type had a significant effect on the quality of data. The single-probe, dual-probe, and multi-probe with braided electrodes performed better than the exposed wire type multi-probe that was placed in three boreholes in S-SX tank farm. However, it is difficult to strictly separate the depth electrode type and method of completion, since the exposed wire multi-probe was completed with no additional moisture in the sand that surrounds the probe.
- **Electrode Placement & Soil Moisture Content:** Antecedent moisture content did not correlate with electrode performance. The moisture at the depth of the electrode was obtained from geophysical logging, and electrodes appeared to be of high quality even when the moisture content was as low as 3 percent. However, the long-term electrode performance within low moisture content zones is unknown.
- **Time from Installation to Use:** There appears to be a time element to performance. When comparing the same type of electrode and completion method (e.g., single and multi-probe depth electrode), longer times between installation and usage equated to better performance. However, the braided wire multi-probe performed extremely well with only three months between installation and usage. A 3 month time window should be sufficient between installation and usage.
- **Electrode Degradation due to Electrolysis:** Some exposed wire multi-probe electrodes were observed to degrade in performance through the survey at S-SX tank farm within a matter of minutes. The resistivity instrument drives current through the transmitting electrodes by controlling the voltage potential across those electrodes. For a given potential, the amount of current output is proportional to the contact resistance of the electrode with the earth. When the meter sensed that current was decreasing, the voltage was increased to compensate. Eventually the voltage was maximized at 400 Volts while

the current continued to decrease. It was suspected that any remaining moisture in the media surrounding these probes was driven off through electrolysis.

- **Limiting Factors:** With the current subset of depth electrodes it was not possible to determine if there are limiting factors for placement. It does not appear that antecedent moisture content affects electrode performance. In addition, the level of infrastructure above the electrode did not degrade the performance.
- **Electrode Spatial Configuration:** From the low quantity of depth electrodes, it is uncertain whether the existing configurations are optimal for long term use, especially for use in resistivity-based retrieval monitoring of waste from the single-shelled tanks. Models that couple hydrological flow simulating a tank leak and electrical resistivity monitoring should be conducted as a first step to test sensitivity of the existing configurations of single-probe, dual-probe, or multi-probe arrays.

Based on these conclusions, the following recommendations should be followed in order to improve data quality for future depth electrode deployments and geophysical surveys:

- Based on the limited number of combinations between installation and usage time, completion methods, and electrode type, we recommend that when moving forward for future deployments of depth electrodes the braided wire mesh multi-probe depth electrode be used with wet diatomaceous material surrounding the probe. It is unknown whether water or salty water added to the diatomaceous material would work best. A three-month time window should be sufficient between installation and usage.
- We recommend that if the single- or dual-probe rod type depth electrodes are to be used, then wet diatomaceous material be used to surround the probe. The diatomaceous material may help decrease the time differential between installation and usage.
- We recommend that longer term studies be conducted on the depth electrodes to understand the potential degradation in performance over time. Monthly or quarterly monitoring surveys could be conducted on a subset of surface electrodes with the depth electrodes to observe changes in output current, repeat error, and reciprocal error. Given that the S-SX tank farm has the most depth electrodes, the monitoring of these electrodes should occur there.
- We recommend that the tabulated results for each new electrical resistivity survey with depth electrodes be added to those presented in Section 3.0 to maintain a base level of knowledge on the depth electrode performance.

5.2 SUBSURFACE CHARACTERIZATION

Results of the data processing analyses through comparisons of more than thirty separate inverse models identified several key features of the electrical resistivity distribution of the subsurface:

- Discrete low-resistivity subsurface targets were identified in the model domain. The main body of these targets appeared to be about 20 to 40 meters bgs. Given the depth of the target, it is likely that infrastructure had minimal effect on the results.
- Using expert judgment, it is believed that the model with surface and depth electrodes, without long electrodes (Model 024) represents the subsurface most accurately. This is

due to the fact that additional subsurface data provided increased sensitivity at depth and gave better resolution to those areas. The model that included wells as long electrodes (Model 026) is suspect, and more research is needed to understand more fully how to incorporate the different data types from surface, depth, and long electrodes together.

- Neutron logging to define volumetric moisture content in the five boreholes, where depth electrodes were placed, shows an increase in moisture at about 25 to 45 meters bgs. The moisture in this region was as high as 30 percent in discrete layers that are about 1 meter thick. Low resistivity targets in the S-SX tank farm area could be attributed to these high moisture regions.

6.0 REFERENCES

CEES-0360, 2007, *Surface Geophysical Exploration System Design Description*, Revision 0, Columbia Energy and Environmental Services Inc., Richland, Washington.

Labrecque and Daily, 2008, "Assessment of measurement errors for galvanic-resistivity electrodes of different composition," *Geophysics*73, F55.

RPP-34690, 2007, *Surface Geophysical Exploration of the B, BX, and BY Tank Farms at the Hanford Site*, Revision 0, CH2M HILL Hanford Group, Inc., Richland, Washington.

RPP-PLAN-45906, 2010, *Work Plan for Surface Geophysical Exploration of the S and SX Tank Farms at the Hanford Site*, Revision 1, Washington River Protection Solutions, LLC, Richland, Washington, Richland, Washington.

RPP-RPT-28955, 2006, *Surface Geophysical Exploration of T Tank Farm*, Revision 0, Prepared by hydroGEOPHYSICS and Columbia Energy and Environmental Services, Inc. for the U.S. Department of Energy, Richland, Washington.

RPP-RPT-41236, 2009, *Surface Geophysical Exploration of UPR 200-E-81 Near the C Tank Farm*, Revision 0, Washington River Protection Solutions, LLC, Richland, Washington.

RPP-ENV-39658, 2010, *Hanford SX-Farm Leak Assessments Report,* Revision 0, Washington River Protection Solutions, LLC, Richland, Washington.

RPP-RPT-42513, 2009, *Surface Geophysical Exploration of the SX Tank Farm at the Hanford Site*, Revision 0, Washington River Protection Solutions, LLC, Richland, Washington.

RPP-RPT-47486, 2010, *Surface Geophysical Exploration of UPR 200-E-86 Near the C Tank*, Revision 1, Washington River Protection Solutions, LLC, Richland, Washington.